Double-diffusive convection in rotating fluids under gravity modulation

School of Computer Science & Applied Mathematics
University of the Witwatersrand

Student: Alfred Mathunyane
Student Number: 1714600
Supervisors: Dr. C T Duba and Prof. D P Mason
Submitted for Masters degree by dissertation.

17 September 2024

Declaration

I hereby declare that this thesis is my work and has been written independently. I have not used any sources or aids other than those indicated, and I have marked every citation accordingly.

Alfred Mathunyane
Date: 17 September 2024

Acknowledgements

I want to express my sincere gratitude to my supervisors, **Dr. C.T. Duba** and **Prof. D.P. Mason**, for their invaluable guidance, support, and mentorship throughout the past two years of my research. Their effectiveness and consistency in pushing me to be a better academic have been commendable. Their expertise, encouragement, and constructive feedback have been instrumental in shaping this study and refining its findings. I am deeply grateful for their unwavering dedication and commitment to excellence, which have undoubtedly enriched my academic journey. Their insights and wisdom have been truly inspirational, and I am privileged to have had the opportunity to learn from their expertise.

Additionally, I extend my heartfelt appreciation to **Dr. W. Carlson** and **Prof. J.R. Moitsheki** for believing in my ability to lecture and allowing me to do so. Last but not least, I would like to thank my aunt **Dr. C.B. Malau** and grandmother **Regina Malau** for all the support throughout this journey.

Abstract

This study employs the method of normal modes and linear stability analysis to investigate double-diffusive convection in a horizontally layered, rotating fluid, specifically focusing on its application to oceanic dynamics. Double diffusive convection arises when opposing gradients of salinity and temperature interact within a fluid, a phenomenon known as thermohaline convection, and it is crucial for the understanding of ocean circulation and its role in climate change. With the increasing mass of water due to glaciers melting, fluid pressure variations occur, leading to slight fluctuations in gravity. We conduct both stationary and oscillatory stability analyses to determine the onset of double-diffusive convection under gravity modulation. Our analysis reveals that time-dependent periodic modulation of gravitational fields can stabilize or destabilize thermohaline convection for both stationary and oscillatory convection, with amplitude stabilizing and frequency destabilizing. The wavenumber in the y- direction also affects convection in the equatorial regions. This wavenumber exhibits destabilizing effects for large values and stabilizing effects for small values for both stationary and oscillatory convection. Rotation along with gravity modulation tends to destabilize the system for both stationary and oscillatory convection. The key difference between stationary and oscillatory convection is that oscillatory convection exhibits large values of the Rayleigh number, thus susceptible to overstability while stationary convection tends to have relatively smaller Rayleigh numbers and thus more stable. This research provides insights into the complex interplay between gravity modulation and thermohaline convection, contributing to our understanding of ocean dynamics and their implications for climate change.

Contents

List of Figures

Chapter 1

Literature Review

1.1 Introduction

Convection is the movement of heat and mass in a fluid due to differences in temperature and density, primarily caused by temperature variations. The study of convection has practical applications in various fields, including geophysical systems, engineering, oceanography, electrochemistry, and solute migration in porous media. Temperature plays a pivotal role in convection, especially when a system is heated from above or below. This heating causes warmer fluids to rise and colder fluids to sink, creating convection currents within the fluid [1]. There are two main types of convection: natural convection, driven by self-induced forces, and forced convection, driven by external forces. Natural convection and forced convection represent distinct modes of heat transfer within fluid mediums. Natural convection arises from density variations due to temperature discrepancies, leading to fluid movement without external intervention. Essentially, as fluid is heated, it becomes less dense and ascends, while cooler, denser fluid descends, generating convective currents [2]. This phenomenon is evident in everyday scenarios, like the rising of warm air above a heat source or the circulation of water in a pot being heated [2]. Conversely, forced convection involves the deliberate movement of fluid induced by external forces, such as mechanical pumps or fans. Unlike natural convection, where buoyancy drives the flow, forced convection relies on external mechanisms to propel fluid through a system. Examples include airflow in fan-forced ovens or water circulation in car engine cooling systems.

The differences between natural and forced convection extend beyond their driving mechanisms to their flow characteristics and applications. Natural convection typically yields slower, more irregular flow patterns, whereas forced convection tends to produce more controlled and uniform flow. Moreover, natural convection commonly finds application in passive heating and cooling systems where temperature differentials drive fluid movement [2]. In contrast, forced convection is integral to actively controlled systems requiring precise regulation of heat transfer, such as those found in industrial processes. While both mechanisms play vital roles in heat transfer, understanding their differences is essential for designing efficient heating, cooling, and ventilation systems that cater to specific needs and environmental conditions [3].

1.1.1 Convection in the ocean and lakes

Ocean convection plays a crucial role in regulating various aspects of the ocean, including heat uptake, water-mass re-distributions, CO_2 exchange, and nutrient transport [4]. This mechanism has significant implications for ocean dynamics and climate change. Surface waters become denser and sink due to the cooling of the atmosphere and salinification from processes like evaporation or sea-ice formation, leading to turbulent convective plumes. Convection deepens and sustains the upper mixed layer of the ocean, with different drivers depending on the region [4]. In tropical and subtropical areas, night-time cooling drives mixed-layer convection, while in mid- and high-latitude regions, winter cooling is the key factor.

Strong convection events occur due to extensive surface heat loss and polynya activity in regions like the sub-polar North Atlantic and the Antarctic continental shelf. These events influence the Meridional Overturning Circulation (MOC) and water-mass transport globally. However, convection is often localized in time and space, posing challenges for accurate measurement in field observations [4]. Global Circulation Models (GCMs) struggle to resolve convection and turbulence, relying on simplified parameterizations that may not fully capture their impact on ocean circulation, air-sea exchange, and biology.

Despite these challenges, there have been significant advancements in observing techniques, numerical simulations, laboratory experiments, and theoretical understanding of ocean convection in recent decades. However, the impacts of climate change on ocean convection are still not fully understood, and key questions remain about future climate scenarios [4].

Inland water bodies like lakes lack tidal influence and experience weaker wind forces compared to oceans, making convective processes pivotal for their mixing and stratification dynamics. The diverse nature of lakes, shaped by local factors like geochemistry, morphology, and meteorology, carries a rich spectrum of convective phenomena, each exhibiting unique characteristics [5]. While traditional studies focus on cooling-induced and shear-induced convections in oceans, lakes feature additional convective processes such as under-ice, sidearm, and double-diffusive convection, alongside thermobaric instability and bio-convection, often overlooked in mainstream research. Furthermore, the density function at lower salinity/temperature values in lakes leaves distinctive imprints [5].

1.2 Rayleigh-Bénard Convection

The investigation of thermal convection dates back to the 1700s when Count Rumford first observed convection currents while experimenting with a large thermometer

[1]. Subsequent experiments by Bénard in the 1900s focused on convective motions in shallow fluid layers [1]. Later, Lord Rayleigh conducted experiments and developed theoretical foundations concerning the dynamics and behavior of fluids in convective processes [1]. He introduced the Rayleigh number (Ra), a dimensionless quantity used to predict the onset of convection. This parameter is expressed as

$$Ra = \frac{g\alpha\beta}{\kappa\nu} d^3, \tag{1.1}$$

where d signifies the layer height, g denotes gravitational acceleration, β (where $\beta = dT/dz$) represents the temperature gradient, while ν, κ, and α correspond to kinematic viscosity, thermal conductivity, and volume expansion coefficients, respectively. The Rayleigh number evaluates the relative impacts of viscosity and buoyancy in a fluid under defined circumstances [1]. His research provides insight into how temperature differentials within a fluid induce motion and mixing. These findings proved to be crucial in understanding convection phenomena such as oceanic currents, atmospheric circulation patterns, and the behavior of fluids in engineering contexts [1]. Due to Rayleigh and Bénard's contributions, thermal convection is now known as Rayleigh-Bénard convection.

In natural convection, instability is found to be due to buoyancy effects when the system is heated from below [1]. Instability theory was discussed in the book by Chandrasekhar [6] and recently by Drazin and Reid [7]. In his groundbreaking research, Chandrasekhar [6] delved into the onset of instability in Rayleigh–Bénard convection, a classical phenomenon observed when a fluid layer heated from below undergoes convective motion. He formulated analytical expressions for critical parameters, notably the critical Rayleigh number, indicating the threshold for convection instability. This parameter, representing the balance between buoyancy and viscous forces, is pivotal in identifying the onset of convective instability. Drazin and Reid [7] extended Chandrasekhar's findings. Their research advances our comprehension of fluid dynamics and heat transfer phenomena, particularly in the realm of instability within convection flow. Their investigations led to the understanding the conditions under which convection flow destabilizes and evolves into complex patterns. A pivotal aspect of Drazin and Reid's work lies in pinpointing critical parameters dictating the stability of convection flows. By examining factors like the Rayleigh number and the Prandtl number, they offer valuable insights into the circumstances triggering instability in convective motion, resulting in the formation of distinctive structures such as rolls, cells, and plumes.

The one common deduction from Chandrasekhar, Drazin and Reid's work on thermal convection instability is that the exchange of instability in convection flows occurs when a stable convective flow becomes unstable, characterized by the emergence of complex flow patterns. This exchange occurs due to various factors such as changes in temperature, fluid properties, or external influences. As the critical parameters governing stability are surpassed, convective motion becomes unstable, leading to the formation of structures like rolls, cells, and plumes. Rayleigh [8] made an important discovery that the system will remain stable if and only if a certain critical number known as the critical Rayleigh number:

$$Ra_c = \frac{27\pi^4}{4} \tag{1.2}$$

is less than or greater than the thermal Rayleigh number (Ra). However, the system will eventually reorder itself to counter this instability. The viscosity and density play a pivotal role in rearranging the system. Understanding this exchange is crucial in fields such as fluid dynamics, meteorology, and engineering, as it influences processes like heat transfer and fluid circulation in natural and engineered systems/forced convection.

This particular manifestation of convection has garnered widespread attention due to its accessibility for experimental and analytical investigation, solidifying its status as one of the most extensively studied classical phenomena.

1.3 Double-diffusive convection

While thermal convection relies on temperature gradients, the recognition of multiple components influencing density became evident in the early 1960s. Henry Stommel, a pioneering oceanographer specializing in ocean circulation and fluid dynamics during that period, proposed an explanatory framework for the mixing and behavioral patterns observed in oceans with varying temperatures and salinity [9]. This phenomenon, where fluid exhibits unexpected behaviors due to temperature and another solute, is now termed double-diffusive convection (or thermosolutal convection) [6]. Double-diffusive convection refers to a convection process where two components with opposing density effects control the fluid density. In the ocean, the convection processes are driven primarily by temperature and salinity differences. The process in which fluids gain or lose heat or salt is known as diffusion. Double diffusive convection can take place due to the opposing diffusion rates of heat and salt. Heat diffuses much faster than salt (approximately 100 times). This form of convection is termed *thermohaline* convection if it is being driven by temperature (thermo) and salt (haline).

Stern [10] initially identified the potential for oscillatory instability when a stable solute distribution compensates for an unstable temperature profile; this leads to enhanced restoring forces and oscillations when warm, salty water is displaced upward. Turner and Stommel's [9] experiments demonstrated that steady convection occurs in systems with thin interfaces separating well-mixed layers, driven by thermal diffusion and moderated by weaker salt diffusion.

In oceanic stability, the notion of the "exchange of instability" is due to the dynamic interaction between stable and unstable fluid motions within the ocean [11]. This exchange occurs due to a variety of factors, including temperature gradients, salinity differences, and external forces, all of which can provoke alterations in the stability of oceanic flows. Within a stable oceanic regime, fluid motions exhibit smooth and well-organized characteristics, with minimal turbulence or disturbances. However, certain conditions, such as temperature gradients or shear forces, can induce instability, giving rise to turbulent eddies, waves, and other dynamic features. Conversely, the exchange of instability encounters scenarios where unstable fluid motions may revert to a stable state [11]. This reversal can be facilitated through mechanisms such as mixing, diffusion, or the dissipation of energy, which serve to reduce turbulent fluctuations and reinstate stability within the flow.

Walin [12] investigated the stability of different thermohaline stratifications, favoring the analysis of the diffusive convection system using classic Rayleigh-Bénard convection, as it provides an accurate analog considering diffusive fluxes through boundaries and cell size proportional to layer depth. Veronis [13, 14] explored finite amplitude behavior through numerical integration, revealing that the presence of solute delays convection onset, but at high Rayleigh numbers, fluxes remain substantial. Noteworthy is the finding that the salt/heat buoyancy flux ratio tends toward -1/2. Nield [15] and Baines and Gill [16] also examined stability under various boundary conditions in such systems. These studies contribute valuable insights into the complexities of diffusive convection and thermohaline.

Due to the extensive applications of double-diffusive convection in industry, significant research has been conducted, with several authors laying foundational work in this field. Researchers such as Chandrasekhar [6], Henry Stommel [9], Veronis [14], Arnold Gordon [17], and Alan Plumb [18] authored numerous papers and books on the subjects of fluid dynamics and oceanography, many of which extensively explored the fundamentals of double-diffusive convection. Their contributions have played a pivotal role in advancing our understanding of this complex phenomenon.

A strong emphasis has emerged on examining the factors influencing convection dynamics, particularly within industrial contexts where understanding the onset of convection holds significance in engineering fields. Bénard's observations, as documented by Chandrasekhar [1], revealed distinctive phenomena:

- A steady flow regime manifested upon heating a plate, characterized by forming regular hexagonal layers.
- The frequency of these patterns, identified as Bénard cells, escalated with increasing depth.
- The spatial separation between these cells expanded as the temperature differential (ΔT) increased [1].

In subsequent investigations of convection, the prominence of double-diffusive convection increased. The industrial sector showed heightened interest in further exploration of double-diffusive convection. Since the 1960s, numerous authors have contributed to the body of literature on double-diffusive convection, establishing a foundational framework for convection research. In recent years, understanding of what affects the onset of double-diffusive convection has grown significantly. Many studies have been conducted to determine how different conditions can affect convection processes. Linden [19] studied a theoretical model for high Rayleigh number double-diffusive convection, characterizing the interface with a dual structure: stable boundary layers producing thermal features at the edges and a diffusive core facilitating molecular transport. It is a time-independent model compared with 'run-down' experiments, viewing each equilibrium state separately. The model predicts a constant buoyancy flux ratio between components, proportional to the square root of their molecular diffusivity ratio, consistent with experimental data. Individual flux estimations align reasonably with observations. Time-dependent aspects are also explored. Overall, the model enhances understanding of double-diffusive convection, particularly in scenarios with high Rayleigh numbers, advancing knowledge applicable in natural and industrial contexts. Hage [20] conducted an experimental setup of an electrodeposition cell to maintain a destabilizing concentration gradient of copper ions in an aqueous solution between its boundaries. This arrangement induces convective motion akin to Rayleigh–Bénard convection. Moreover, the cell imposes a stabilizing temperature gradient despite being significantly weaker than the chemical buoyancy. Interestingly, even with thermal buoyancy much smaller than chemical buoyancy, the presence of this gradient greatly influences the convection pattern, resulting in the formation of double-diffusive fingers consistently across cases.

The size and velocity of these fingers remain unaffected by the cell's height but are contingent upon the concentration difference of ions between the boundaries and the applied temperature gradient. The observed scaling of mass transport aligns with prior findings on double-diffusive convection. Overall, the study sheds light on the complex interaction between concentration gradients, temperature differentials, and convective motion in electro-deposition cells, offering valuable insights into their behavior and potential applications. McDougal [21] conducted the study of double-diffusive convection in scenarios where a significant coupled diffusion effect is present, exemplified by the Soret effect, where solute flux depends on its gradient and the temperature gradient. Extending linear stability analysis to include cross-diffusion flux terms reveals that finger-like structures can develop under substantial coupled diffusion effects even when both solute concentrations yield statically stable density gradients. A comparison of conditions for diffusive instability and finger formation highlights their mutual exclusivity in specific linear property gradients. Additionally, the text explores finite-amplitude, steady, infinitely long fingers, demonstrating that substantial cross-diffusion effects can sustain them even when solute concentrations increase with depth. Furthermore, it shows that property diffusion from an initially sharp interface can establish favorable vertical gradients conducive to finger formation. This comprehensive examination deepens our understanding of the interplay between diffusion effects and finger formation in double-diffusive convection.

The hydrodynamic equations governing convection flows are often derived through the Boussinesq approximation, simplifying density considerations to the buoyancy term [6]. A prevalent assumption postulates a linear relationship between temperature and density [6]. The Boussinesq approximation reduces the momentum equation, allowing for possible analytical solutions [7]. Numerous applications of this approximation in Rayleigh-Bénard convection have been documented [7].

Yoshida and Kagayama [22] devised novel numerical methods, such as the "Yin-Yang grid" technique, to address thermal convection under the Boussinesq approximation. Their methodological innovation facilitated the examination of mantle convection in planetary systems [22]. Rayleigh employed the Boussinesq approximation in analyzing Bénard cells in 1916 [23]. Spiegel and Veronis [23, 13] revisited the assumptions underlying convection studies in incompressible fluid layers, validating constraints on vertical dimensions and fluctuations in pressure and density. They further discerned two stable solutions at low Rayleigh numbers.

1.4 Rotation in convection flows

When rotation is incorporated into convective systems, it fundamentally alters flow dynamics and patterns, particularly notable in geophysical and astrophysical contexts where celestial body rotation influences fluid motion [24]. Rotation induces the Coriolis force, causing the motion to deflect in opposite directions between the Northern and Southern Hemispheres, contributing to large-scale circulation patterns like Earth's Hadley cells or planetary zonal flows [24].

Moreover, variations in fluid density or temperature under rotation can generate Rossby waves, which are significant in atmospheric and oceanic circulation, shaping weather and climate dynamics [25]. In rapidly rotating systems, like Earth's core or gas giants' atmospheres, the Taylor-Proudman theorem asserts fluid motions align predominantly with the rotation axis, forming cylindrical columns with minimal perpendicular variation [26]. This interplay between rotation and convection leads to diverse flow phenomena, from large-scale circulation to small-scale turbulence, critical for understanding geophysical processes, astrophysical phenomena, and engineering applications.

Various studies have been conducted on the effects of rotation in convection. Julian et al [27] studied turbulent Boussinesq convection under rapid rotation, where rotation occurs on timescales comparable to convection. The transition to turbulence follows a clear sequence, beginning with unstable convection at moderate Rayleigh (Ra) and Taylor (Ta) numbers, and progressing to a regime characterized by coherent plume structures at high Ra and Ta. The Taylor number is given by

$$Ta = \frac{4\Omega^2 d^4}{\nu^2}$$

where, Ω is the angular velocity, d is the characteristic length scale, and ν is kinematic viscosity. Similar to non-rotating scenarios, the rapidly rotating state demonstrates a simple power-law relationship with Ra for statistical flow properties. Heat transport scales as 10^7 with no-slip boundaries, akin to non-rotating experiments, but transitions to a different law at $Ra = 4 \times 10^7$ with stress-free boundaries. Due to angular momentum conservation, plume structures at heated and cooled boundaries undergo cyclonic spin-up, leading to vortex-vortex interactions that modify the flow state and result in a finite background temperature gradient as Ra tends to infinity while the ratio between the Rayleigh number and Taylor number remains constant.

The study of rotation on convection dates back to the early 1950s [28]. Most of the research is on the rotating Rayleigh-Bénard convection. Researchers such as [25], [28],

[29] and [30] all studied rotating convection on the Rayleigh-Bénard convection all following the *traditional approximation* (TA) on the angular velocity, Ω. In this approximation, only the x-component of the angular velocity is taken into consideration and the y-component is ignored.

The traditional approximation of angular velocity is a simplification used in geophysical fluid dynamics, especially for studying rotating systems such as oceans and atmospheres [31]. It assumes that the Coriolis force, resulting from the Earth's rotation, mainly influences horizontal motion. In this approximation, only the component of the Earth's rotation vector perpendicular to the local vertical is considered, while the vertical component is ignored [31]. This simplification effectively analyzes large-scale flows where horizontal movements are much more significant than vertical ones. The traditional approximation of angular velocity, while simplifying the study of rotating geophysical systems, comes with several drawbacks [31]. Although this approximation is reasonable, it can lead to inaccuracies in regions with significant vertical motions, such as deep ocean currents or near the poles. This limitation restricts the approximation's applicability primarily to large-scale, low-latitude flows, and it may result in errors when applied near the equator or in areas with rapid changes in the Coriolis force [31]. Additionally, the approximation can distort the behavior of wave propagation, particularly for internal gravity and it may reduce accuracy in shallow water where vertical gradients play a crucial role.

In a rotating system, the Coriolis and the centrifugal forces affect the inertial equations. The centrifugal force is a type of force that acts on a rotating body in the direction away from the body. At the same time, the Coriolis force is a type of force that reacts perpendicular to the direction of motion in a rotating system. Previous studies on thermal and double-diffusive convection under rotation assume the traditional approximation of the angular velocity vector by neglecting the cosine term of the vector [31]. However, in this work, we will consider the cosine term.

Duba et al [32] examined thermohaline convection within a rotating fluid layer in the context of ocean dynamics. The research demonstrated that rotation acts to stabilize the system, while temperature exerts a destabilizing influence. For oscillatory convection, the analysis becomes critical, as the Rayleigh number becomes dependent on six parameters. Through graphical representation, the study showed the interplay among these parameters. Notably, it suggested that the salinity Rayleigh number, Lewis number, and rotation serve to delay instability. These results provided fresh insights into the behavior of large-scale fluids, particularly concerning weakly nonlinear stability.

The study of rotation on the onset of convection in the solar system is significant because it helps us understand how heat radiates. The heat generated in the solar interior drives the resulting convective motions. Like the Sun, giant planets (Jupiter, Neptune, and Saturn) possess convecting outer layers. But the giant planets rotate faster than the Sun. They generate strong alternating zonal jets in their atmospheres. In contrast, the Sun has only one zonal jet because of its weak rotation.

Convection in the ocean is very different from that of the Sun and the giant planets in terms of the driving forces of convection in the ocean and on the Sun and the giant planets. The driving force in the ocean is due to spatially varying and temporal cooling due to seasonal changes in atmospheric conditions, while that of the Sun and the giant planets is heat generated in the solar interior. Thus, oceanic convection is somewhat time-dependent [27]. These convections are complicated due to the problems introduced by rotation. It is also interesting to note that all these convections have very high Reynolds

$$Re = \frac{UL}{\nu},$$

and low Rossby numbers,

$$R_0 = \frac{U}{Lf},$$

thus implying rotationally constrained convictions. Here, U represents flow velocity, L is a characteristic length, ν is the kinematic viscosity, and f is the Coriolis parameter, which is defined as $f = 2\Omega\ \sin\theta$, where Ω is the angular velocity of the Earth, and θ is the latitude. In contrast, our planet's atmosphere has a large Rossby number, R_0. Thus, rotation cannot be ignored [27].

At high altitudes, small-scale convections occur in the ocean due to differences in buoyancy and temperature flux on the ocean surface [24]. The existence of planetary rotation affects horizontal geostrophic circulation. For convection with rotation, it is found that for large Rayleigh numbers, potential energy is released and leads to turbulent mixing [24]. The kinematic equations for such a convection problem are principally different from those of the Rayleigh-Bénard and thermohaline convection [24].

1.5 Modulation in double-diffusive convection

The study of fluid instabilities becomes apparent thanks to the vast knowledge of convection and double-diffusive convection. In convective processes, it is important to understand when instability will occur. This behavior is known as the onset of convection [6]. The onset of convection depends on various parameters such as rotation, temperature, gravity, and salinity [32]. Varying one of the parameters can change the onset of convection. This phenomenon is known as modulation. Many studies have been conducted to understand the role of different modulations. Venezian [33] investigated the stability of a horizontal layer of fluid heated from below under steady temperature differences between the walls, with the introduction of a time-dependent sinusoidal perturbation to the wall temperatures. Results indicate the potential to either speed up or postpone the onset of convection through time modulation of the wall temperatures.

Modulation is essential within double-diffusive convection, influencing various faces of this complex fluid phenomenon [6]. Firstly, modulation enhances mixing within the system by inducing the creation of distinct structures like fingers or layers [10].

These structures facilitate the exchange of heat and solute across different fluid regions, thereby intensifying mixing processes crucial for fluid transport in oceans and enhancing heat transfer efficiency in industrial setups [34]. Secondly, modulation contributes to both stability and instability within the system. It can stabilize the flow by organizing it into well-defined structures that resist perturbations while driving instabilities such as fingering or layering, which drive convective motion and amplify mixing dynamics [34].

Furthermore, modulation significantly impacts transport processes occurring within the fluid, altering the rates of heat and mass transfer. Modulation modifies the driving forces for diffusion and convection by inducing spatial variations in temperature and concentration, resulting in complex transport patterns and mixing [10]. This modulation-driven interplay between diffusive and advective processes ultimately leads to distinctive patterns observed in double-diffusive convection, such as the spatial distribution of fingers, layers, or convective cells [10].

Understanding the role of modulation in double-diffusive convection holds practical significance across various applications [34]. It highlights crucial processes in ocean circulation models, heat exchange design, and geophysical fluid dynamics [34]. By understanding the underlying mechanisms and behaviors influenced by modulation, researchers can optimize processes and accurately predict the behavior of complex systems. In summary, modulation emerges as a fundamental mechanism shaping double-diffusive convection dynamics and behavior, profoundly impacting mixing, stability, transport processes, pattern formation, and practical applications across diverse fields [34].

Modulation in double-diffusive convection holds significant importance across various scientific and industrial domains. Firstly, in ocean circulation, where different water masses of varying temperatures and salinities interact, double-diffusive convection plays a crucial role, particularly in deep thermohaline circulation patterns [34]. Understanding modulation helps in unpacking these circulation dynamics, which are pivotal for global climate and weather patterns. Moreover, modulation influences biological productivity in aquatic ecosystems by affecting nutrient distribution [35]. The mixing processes driven by double-diffusive convection determine the availability of nutrients and dissolved gases, directly impacting the growth and distribution of marine organisms [34].

In oil and gas exploration industries, knowledge of modulation in double-diffusive convection is critical for predicting fluid behavior in geological formations [36]. This understanding is essential for optimizing extraction techniques and maximizing resource recovery rates. Furthermore, in climate modeling, double-diffusive convection contributes to the atmosphere's heat and mass transfer processes, affecting cloud formation, precipitation patterns, and greenhouse gas distribution [35]. Accurate representation of modulation in climate models is critical for improving predictions of future climate change scenarios.

Lastly, modulation in double-diffusive convection has practical implications in engineering applications [7]. It influences heat and mass transfer rates in crystallization, desalination, and heat exchanger performance, impacting various fields, including chemical processing, material science, and environmental engineering [34]. Understanding modulation in double-diffusive convection is essential for understanding a wide range of natural and engineered systems, from global climate dynamics to industrial processes, resource management, and environmental sustainability.

1.5.1 Gravity modulation on convection

The influence of gravity on convection remains a subject that needs to be thoroughly studied within scientific discourse. Understanding natural convection in environments like the ocean without the Earth's gravitational field poses significant complexities due to gravity's pivotal role as the driving force for such phenomena [3]. Gravity modulation is highly influential in addressing large-scale convection problems, particularly in oceanic contexts. Similar to temperature modulation, the modulation of gravity offers a means to regulate convection [37].

Interest in the impact of gravity modulation on convection has escalated over time, paralleling the burgeoning curiosity among researchers regarding convection currents in oceanic systems. These currents, fundamental to oceanic convection, arise predominantly from density disparities attributed to temperature and salinity variations in the ocean. The interplay of temperature and salinity engenders opposing diffusivities, which, in turn, sustain the convection currents. Despite considerable investigation, the influence of gravity modulation on convection remains ripe for exploration.

Studies have highlighted the effects of gravity modulation on Rayleigh-Bénard convection, focusing on its implications in various specialized scenarios. Vadasz [38], for instance, employs linear stability and weak nonlinear theories to investigate the influence of the Coriolis effect on three-dimensional gravity-driven thermal convection occurring within a rotating porous layer that is heated from below employing the traditional approximation on rotation. Notably, he discovers that overstable convection in porous media is not constrained to specific Prandtl number, $Pr = \nu/\kappa$, ranges unlike in non-porous fluids where the Prandtl number must be greater than one. Additionally, the critical wavenumber for stationary convection in porous media differs from that in non-rotating situations, a distinction absent in non-porous fluid systems.

Despite these differences, the study reveals that high viscosity in porous media destabilizes stationary convection, aligning with similar effects observed in non-porous fluids under rotation. Weak nonlinear analysis yields differential equations for amplitude, revealing pitchfork bifurcation for stationary convection and Hopf bifurcation for overstable convection. Heat transfer assessments, derived from amplitude solutions, express Nusselt number, Nu variations for both types of convection. Rotation generally hinders convective heat transfer, except for a narrow range of low Prandtl number values where rotation enhances heat transfer in overstable convection scenarios.

The study shows the interplay between rotation, porous media, and gravity-driven convection, highlighting critical insights into such systems' stability and heat transfer dynamics. Moreover, investigations by Malashetty and Padmavathi [39] explored gravity modulation's role in the onset of thermal convection. A linear stability analysis was conducted to demonstrate the substantial influence of gravity modulation on the stability of thermal convection. Employing Venezian's method for small modulations, the critical values of Rayleigh number and wavenumber were computed. The variation in critical Rayleigh number was assessed with respect to the modulation frequency and Prandtl number. The analysis revealed that low-frequency modulation can impact the system's stability. Bhadauri and Kiran [40] studied convective instability in an electrically conducting fluid, shedding light on how adjustments in gravity modulation parameters can govern heat and mass transfer.

Further research endeavors, such as Kiran et al. [41, 42], studied the interplay between gravity modulation and various convection phenomena, uncovering important relationships. These investigations highlighted factors influencing heat transfer and the transition from steady to chaotic thermal convection, underscoring the crucial dynamics governed by gravity modulation. Kiran [43] examined the impact of gravity modulation on Rayleigh–Bénard convection under rigid isothermal boundary conditions, he utilized insights from the Ginzburg–Landau equation (GLE). His investigation considered gravity modulation comprising both steady and sinusoidal components. Specifically, the sinusoidal aspect characterized gravity modulation in terms of its amplitude and frequency. The findings illustrate that gravity modulation dictates the outcomes of heat transfer. Notably, the amplitude of modulation amplifies heat transfer at lower frequencies while attenuating it at higher frequencies.

In the realm of physics, the gravitational pull of objects is well-understood to be proportional to their mass. Examination of pressure variations in the ocean offers insights into oceanic circulation and gravitational fluctuations. Regions experiencing elevated pressure manifest more vital gravitational forces, particularly evident in denser areas. Variations in mass concentrations, such as those resulting from glacier melting, induce corresponding alterations in bottom pressure and gravitational fields across the ocean.

The average gravitational acceleration on Earth, approximately $9.8\,m/s^2$, exhibits slight variations based on location, with discernible differences between equatorial and polar regions. Despite their modest magnitudes, these variations play a pivotal role in analyzing oceanic convection currents. The temporal manifestation of gravitational changes may span weeks to months, influenced by processes such as ocean floor heating and glacier melting, which unfold over extended time frames.

A time-dependent periodic function is the most commonly used form of the gravity modulation equation in the convection field. Bhadauri and Kiran [44] employed the equation

$$g(t) = g_0(1 + \delta \cos \omega t), \tag{1.3}$$

while Kiran et al. [41] utilized the equation

$$g(t) = g_0(1 + \delta \sin \omega t). \tag{1.4}$$

In summary, the interplay between gravity modulation and convection processes, particularly in oceanic contexts, underscores the complexity inherent in understanding and predicting natural phenomena governed by gravitational dynamics. Ongoing research efforts continue to illuminate the multifaceted relationships shaping convection patterns in diverse environmental settings.

1.6 Motivation of research

The drive for this research arises from the reassessment of three components: the escalating ocean temperatures, variations in gravity at the ocean bottom, and the departure from traditional approximations (TA) of the Coriolis effect [31]. Over recent years, there has been a notable rise in ocean temperatures, contributing to destructive natural phenomena such as El Niño. In the past four decades, the average ocean temperature has increased by $0.6°$C [31]. A recent NASA study concluded that as the oceans experience warming, there are alterations in the transport and exchange of mass and heat [31].

Temperature increase facilitates glacier melting. The melting of glaciers introduces cold freshwater into the ocean, leading to large-scale mass redistribution. This phenomenon enables different regions to experience varying gravitational forces. Additionally, temperature increase typically destabilizes the convection process. Recent studies have highlighted variations in gravitational effects on the ocean bottom [45]. Particularly noteworthy is the 2002 launch of two NASA satellites—one dedicated to gravity recovery and the other for climate experiments. Over nearly 12 years, these satellites aimed to measure the average gravitational field and monthly variations in gravity within wavelengths ranging from 300 to 4000 km. They utilized a time-dependent variation in mass and gravity for the ocean, allowing for the assessment of variations in mass distributions relative to gravitational fluctuations in the ocean [45].

For over a decade, researchers have embraced the concept that the Coriolis force can be partially accounted for by omitting the components proportional to the cosine of latitude [46]. This concept is referred to as the traditional approximation (TA) of the Coriolis effect, originally proposed by Laplace in 1878 [46]. The (TA) predominantly influences deep convection, Ekman spirals, internal waves, and equatorial jets. The concept behind the traditional approximation is to have the Earth's angular velocity vector predominantly aligned with the vertical z-axis. That is,

$$\mathbf{\Omega} = \Omega \sin \theta \mathbf{k}. \tag{1.5}$$

The literature indicates that many researchers employ the traditional approximation (TA) of the Coriolis effect when investigating stability in rotating convection flows. This study aims to delve into the unexplored territories of nontraditional approximation. We incorporate the cosine term into the equation (1.5). By doing so, we express the angular velocity ($\mathbf{\Omega}$) of the Earth as:

$$\mathbf{\Omega} = \Omega\cos\theta\mathbf{j} + \Omega\sin\theta\mathbf{k}. \tag{1.6}$$

Thus, disregarding the cosine term in Ω, (TA approximation) results in convective plumes becoming tilted, dependence on wind direction emerges in Ekman spirals, and numerous alterations occur in internal wave behavior [31]. These changes include the presence of trapped low-frequency waves and an expansion of their habitat towards the poles. In the astrophysical domain of stars and gas giant planets, the traditional approximation (TA), influences patterns of thermal convection and the rate of tidal dissipation [31].

Aims and objectives of research

This research aims to conduct a linear stability analysis in a horizontal fluid layer heated from below in a rotating frame of reference. We employ a Boussinesq approximation. This approximation simplifies the governing equations by assuming that density variations are negligible except where they appear in buoyancy forces, allowing for an accurate yet manageable fluid flow analysis. The specific objectives of this study are to:

- Derive equations governing double-diffusive convection under the Boussinesq approximation for a horizontal layer of fluid heated from below
- Determine the relevant boundary conditions in the case when the x and y components of the Coriolis effect are taken into consideration.
- Employ normal modes to determine the critical Rayleigh number for stationary convection.
- Conduct the stability analysis by varying the frequency and amplitude of gravity and other parameters to determine their impact on oscillatory convection.

1.7 Summary

In summary, this chapter provides foundational background on double-diffusive convection, modulation in convection such as gravity modulation, convection in rotating fluids, and the traditional approximation of angular velocity. In this work we will employ the non-traditional approximation where we consider both horizontal and vertical motion since we will consider thermohaline convection across different altitudes.

This research is subdivided into the following chapters. Chapter 1 reviews the different literature on double-diffusive convection and Chapter 2 describes the method of normal modes. The mathematical model is developed in Chapter 3 whereas Chapter 4 prepares us for linear stability analysis using the method of normal modes. Chapter 5 is concerned with stationary convection and Chapter 6 considers oscillatory convection analysis. Lastly, Chapter 7 summarizes and concludes our results.

Chapter 2

Methodology

2.1 Introduction

The preferred methodology is the utilization of the normal modes technique. A normal mode represents a form of motion in which constituent elements of a system exhibit sinusoidal motion at an identical frequency. These motions transpire at fixed frequencies, commonly called resonant frequencies or natural frequencies. In the context of physical structures, the characteristics of normal modes are dependent upon the specific material employed and the boundary conditions applied. In musical instruments that generate vibrations, these modes are termed “overtones” or “harmonics.” The superposition of normal modes is a critical phenomenon in various systems, and these modes act independently of each other.

2.2 Method of normal modes

Recent studies have applied both numerical and direct methods to normal modes. Scholars have devoted substantial attention to exploring linear and nonlinear normal modes in recent years. Numerous attempts to determine these modes have been conducted spanning from the 1960s to the present. In these endeavors, Platzman [47] employed the method of normal to study the Rayleigh-Bénard convection by transforming the problem to the spectral domain and applying numerical methods to the resulting equations. Vakakis [48] made noteworthy contributions by using the method of normal nodes on Manevich and Mikhlin’s [49] perturbation methodology along with the method of multiple scales [50]. Additionally, Drazin and Reid [7] investigated the stability problem rooted in Rayleigh’s work by employing the method of normal modes. Numerous studies on thermal convection stability have been conducted utilizing the method of normal modes.

In double-diffusive convection, Duba et al [32] employed the method of normal modes to study the effect of the Soret and Dufour effects in a rotation thermohaline convection using the traditional approximation for the angular velocity. Mirouh [51] utilized the method of normal modes to investigate double-diffusive convection on Earth and planetary sciences assuming the traditional approximation. Shankar [52] investigated the stability of a primary buoyant flow in a vertical layer of fluid. The flow density is controlled by temperature and solute concentration. The method of normal modes was employed. The resulting equations were solved numerically using the Chebyshev collocation method.

The literature shows that the normal modes method is widely utilized to study convection stability under various conditions. Rayleigh [8] investigated the stability and instability of a Boussinesq fluid subject to thermal convection. In his pursuit of stability analysis, Rayleigh employed the normal modes method. Rayleigh's investigation focused on a fluid confined between two infinite horizontal plates, each heated from below at dissimilar temperatures.

2.3 Application of the method of normal modes

In applying the normal mode method, Chandrasekhar [1] considered a fluid confined between two infinite horizontal layers heated from below at different temperatures (T_0 and T_d). Let d be the distance between the two layers. The lower layer serves as the origin for the Cartesian plane. The z-axis is perpendicular to the two layers. Under appropriate transformations, the linear stability equations are given by the following non-dimensional equation,

$$\frac{\partial \mathbf{q}}{\partial t} = -Pr\nabla p + T\ Pr\ Ra\ \mathbf{k} + Pr\ \nabla^2\mathbf{q}, \tag{2.1}$$

the continuity equation

$$\nabla \cdot \mathbf{q} = 0, \tag{2.2}$$

and the temperature gradient

$$\frac{\partial T}{\partial t} - w = \nabla^2\ T, \tag{2.3}$$

where $\mathbf{q} = (u, v, w)$ is the velocity vector, $\mathbf{k}$ is the basis vector in the z direction, T is the temperature, p is the pressure, α is the volumetric expansion due to temperature differences, κ is the heat diffusion coefficient, g is the gravitational acceleration, ν is the kinematic viscosity,

$$Ra = \frac{g\alpha\Delta T d^3}{\kappa\nu}$$

is the dimensionless Rayleigh number and

$$Pr = \frac{\nu}{\kappa}$$

is the Prandtl number which describes the ratio between the momentum diffusivity to the thermal diffusivity. Taking the curl of equation (2.1) we get the following

$$\frac{\partial \boldsymbol{\sigma}}{\partial t} = Ra\ Pr\ (\nabla T \times \mathbf{k}) + Pr\ \nabla^2\boldsymbol{\sigma}, \tag{2.4}$$

where $\boldsymbol{\sigma} = \nabla \times \mathbf{q}$ is the vorticity. In particular, the z-component of the curl of equation (2.4) is given by

$$\frac{\partial}{\partial t}(\nabla^2 w) = Pr\ Ra\nabla^2 T + Pr\nabla^2 w, \tag{2.5}$$

where $\nabla_H^2 = \frac{\partial^2}{\partial x^2} + \frac{\partial^2}{\partial y^2}$ is the horizontal Laplacian and Δ. Eliminating T from (2.3), we obtain

$$\left(\frac{\partial}{\partial t} - \nabla\right)\left(\frac{1}{Pr}\frac{\partial}{\partial t} - \nabla\right)\nabla w = Ra\ \nabla^2 w. \tag{2.6}$$

We then impose the boundary conditions that is,

$$w = \frac{\partial w}{\partial z} = T = 0 \quad (\text{rigid} \quad \text{boundary}) \ \text{ at } \ z = 0, \tag{2.7}$$

$$w = \frac{\partial^2 w}{\partial z^2} = T = 0 \quad (\text{free} \quad \text{boundary}) \ \text{ at } \ z = d. \tag{2.8}$$

The various cases are called *rigid-rigid, rigid-free, free-rigid, or free-free* according to whether the upper and lower boundaries are free or rigid.

Equations (2.3, 2.4, 2.7 and 2.8) are symmetric in x and y. Thus Rayleigh managed to take normal modes of the form

$$w = W(z)f(x,y)e^{st} \text{ and } T = T(z)f(x,y)e^{st}, \tag{2.9}$$

where $s = \delta + i\sigma$ is the growth rate. Therefore, equation (3.3) becomes

$$(D^2 - \nabla - s)fT(z) = -fW, \tag{2.10}$$

where $D = \frac{d}{dz}$. Therefore,

$$(D^2 - a^2 - s)T(z) = -W, \tag{2.11}$$

and

$$\nabla^2 f + a^2 f = 0, \tag{2.12}$$

where a^2 is the constant of separation. Equation (2.12) is known as the membrane equation, Helmholtz equation, or the reduced wave equation. Thus, a can be taken as the wave number.

The variations of the solution in z are given by,

$$(D^2 - a^2)(D^2 - a^2 - s/Pr)W = a^2 Ra\ T, \tag{2.13}$$

and

$$(D^2 - a^2)(D^2 - a^2 - s)(D^2 - a^2 - s/Pr)W = -a^2 Ra\ W, \tag{2.14}$$

where

$$Ra = \frac{g\alpha\beta d^4}{\kappa\nu}.$$

The solution to the equations is not trivial. So for given values of $Ra,\ a$ and Pr, a set of solutions W_i that satisfy the boundary conditions is needed to represent the initial disturbance. For given values of Pr and Ra the flow is unstable for $\delta > 0$, for any mode with any real value a, and stable if $\delta \leq 0$ for all modes. The critical Rayleigh number is the value Ra_c for which $\delta(Ra, a, Pr)$ for some a whenever $Ra > Ra_c$ and $\delta(Ra, a, Pr) \leq 0$ for all a whenever $Ra \leq Ra_c$. For $\sigma = 0$, $s = \delta$ thus creating a stationary convection process, and for $\sigma \neq 0$, the growth rate creates an oscillatory motion.

2.4 Summary

This chapter provides insight into the method of normal modes. The method of normal modes offers a simplification of complex systems, insight into natural frequencies, decoupling of equations, reduced computational load, and many other advantages. In this dissertation, we apply the method of normal modes while expressing our angular velocity Ω in terms of both the horizontal components Ω_x and Ω_y and assuming variable gravity in a rotating system. The method of normal modes in convection analysis aims to determine the stability of a fluid system by breaking down disturbances into sinusoidal modes or waves. By analyzing these modes, the method identifies which disturbances grow or decay over time. If a mode grows, the system is unstable and likely to lead to convection; if it decays, the system remains stable. This approach helps in understanding the conditions under which convection occurs and the nature of the resulting flow patterns.

Chapter 3

Mathematical Model

3.1 Introduction

In this chapter, we derive the equations of motion to describe the fluid flow in a horizontal layer heated from below with salinity in the system. These include the continuity equation, momentum equation, temperature equation, salt equation, and the equation of state. In deriving the governing equations, we assume familiarity with the results of the divergence theorem, the stress tensor matrix, and Fourier's law of heat conduction. This set of equations will be analyzed in the next chapter. The divergence theorem states that the total flow of a vector field out of a closed surface is equal to the sum of the field's sources and sinks inside the enclosed volume. In mathematical rotation,

$$\int_S \mathbf{F} \cdot \mathbf{n} \, dS = \int_V \underline{\nabla} \cdot \mathbf{F} \, dV, \tag{3.1}$$

where S is a closed surface with unit upward normal $(\mathbf{n})$, $\mathbf{F}$ is a vector field and V is the volume. In index notation,

$$\int_S F_k n_k \, dS = \int_V F_{k,k} \, dV, \tag{3.2}$$

where comma notation denotes partial differentiation,

$$F_{k,k} = \frac{\partial F_k}{\partial x_k}. \tag{3.3}$$

The divergence theorem can be extended to tensor T of any order,

$$\int_S T n_k \, dS = \int_V T_, k \, dV, \tag{3.4}$$

where T has any arbitrary number of indices, not necessarily the index k. The Cauchy stress tensor is,

$$\tau_{ij} = \begin{pmatrix} \tau_{xx} & \tau_{xy} & \tau_{xz} \\ \tau_{yx} & \tau_{yy} & \tau_{yz} \\ \tau_{zx} & \tau_{zy} & \tau_{zz} \end{pmatrix}, \tag{3.5}$$

where τ_{ij} is the stress tensor matrix. It follows from the principle of angular momentum that the Cauchy stress tensor is symmetric,

$$\tau_{ij} = \tau_{ji}. \tag{3.6}$$

The components of the stress tensor are given by

$$\tau_{yx} = \mu \left(\frac{dv_x}{dy} + \frac{dv_y}{dx} \right), \ \tau_{yz} = \mu \left(\frac{dv_z}{dy} + \frac{dv_y}{dz} \right), \text{ and } \tau_{zx} = \mu \left(\frac{dv_z}{dx} + \frac{dv_x}{dz} \right). \tag{3.7}$$

Let $\mathbf{H}$ be the heat flow vector. Then Fourier's law of heat conduction is given by

$$\mathbf{H} = -\kappa \underline{\nabla} T, \tag{3.8}$$

where κ is the material heat conduction and T is temperature.

From Newton's law of friction, consider the velocity of the fluid (called the fluid velocity). The fluid velocity at time t is denoted by $\mathbf{v}(\mathbf{r}, t)$, where $\mathbf{r}$ is the position vector. Consider the Cartesian coordinates (x, y, z). Define $\mathbf{i}$, $\mathbf{j}$, $\mathbf{k}$ to be mutually orthogonal unit vectors in R^3. Thus $\mathbf{r}$ and $\mathbf{v}$ can be expressed as

$$\mathbf{r} = x(t)\mathbf{i} + y(t)\mathbf{j} + z(t)\mathbf{k}, \tag{3.9}$$

and

$$\mathbf{v} = v_x\mathbf{i} + v_y\mathbf{j} + v_z\mathbf{k}, \tag{3.10}$$

where

$$v_x = \frac{dx}{dt}, \qquad v_y = \frac{dy}{dt}, \qquad \text{and} \qquad v_z = \frac{dz}{dt},$$

and

$$v_x = v_x(x, y, z, t), \qquad v_y = v_y(x, y, z, t), \qquad \text{and} \qquad v_z = v_z(x, y, z, t).$$

The flow is steady if

$$\frac{\partial \mathbf{v}}{\partial t} = \mathbf{0}.$$

Consider now the time rate of change following the motion of the fluid. Let $f(x, y, z, t)$ be a continuum variable. Then $\frac{\partial f}{\partial t}$ is the rate of change of f at a point and $\frac{Df}{Dt}$ is the time rate of change following the motion of the fluid. Then,

$$\frac{Df}{Dt} = \frac{\partial f}{\partial x}\frac{dx}{dt} + \frac{\partial f}{\partial y}\frac{dy}{dt} + \frac{\partial f}{\partial z}\frac{dz}{dt} + \frac{\partial f}{\partial t}, \tag{3.11}$$

thus

$$\frac{Df}{Dt} = \frac{\partial f}{\partial t} + (\mathbf{v} \cdot \underline{\nabla}) f. \tag{3.12}$$

The acceleration of a fluid at position $\mathbf{r}$ is given by,

$$\frac{D\mathbf{v}}{Dt} = \frac{D}{Dt}(v_x\mathbf{i} + v_y\mathbf{j} + v_z\mathbf{k}), \tag{3.13}$$

which can be expressed as,

$$\frac{D\mathbf{v}}{Dt} = \frac{Dv_x}{Dt}\mathbf{i} + \frac{Dv_y}{Dt}\mathbf{j} + \frac{Dv_z}{Dt}\mathbf{k}. \tag{3.14}$$

Using equation (3.12), we can now have

$$\frac{D\mathbf{v}}{Dt} = \left(\frac{\partial v_x}{\partial t} + (\mathbf{v}\cdot\underline{\nabla})v_x\right)\mathbf{i} + \left(\frac{\partial v_y}{\partial t} + (\mathbf{v}\cdot\underline{\nabla})v_y\right)\mathbf{j} + \left(\frac{\partial v_z}{\partial t} + (\mathbf{v}\cdot\underline{\nabla})v_z\right)\mathbf{k}, \tag{3.15}$$

thus,

$$\frac{D\mathbf{v}}{Dt} = \frac{\partial \mathbf{v}}{\partial t} + (\mathbf{v}\cdot\underline{\nabla})\mathbf{v}. \tag{3.16}$$

Equation (3.16) is the acceleration of a fluid element following the motion of the fluid.

3.2 Equations of incompressible fluid

Consider a fluid flow between two semi-infinite horizontal layers heated from below. The density of the fluid in the system is primarily affected by changes in salt and temperature. Let T_0 and S_0 be the initial temperature and salt in the system, d the height

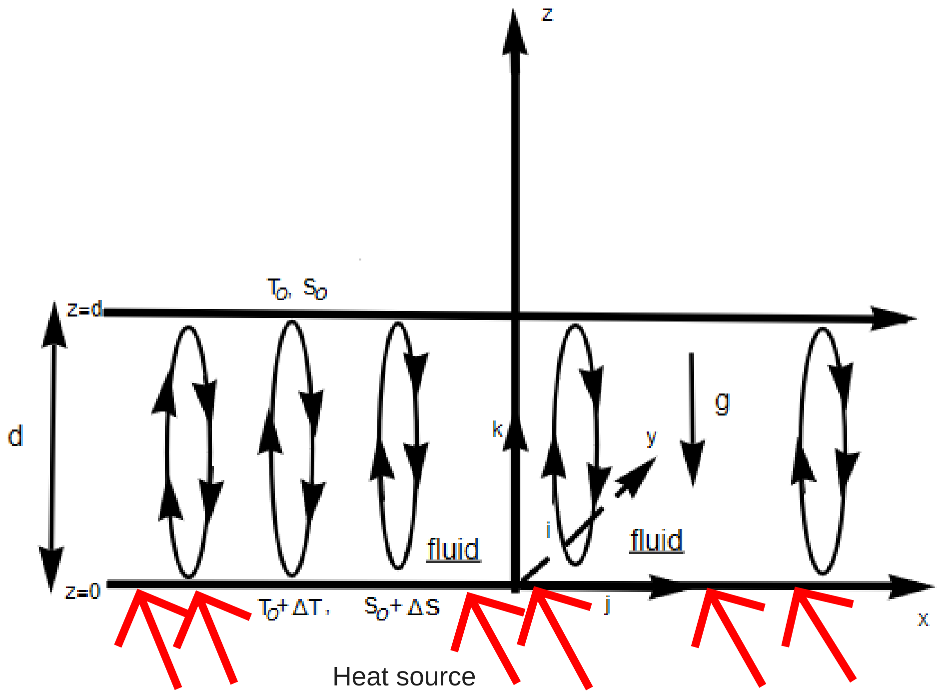

Figure 3.1: *Double diffusive convection process where salt and temperature are the main diffusers.*

between the two horizontal layers, g is the gravitational acceleration, and the boundary conditions at $z = 0$ and $z = d$ are given by,

$$T(z=0) = T_0 + \Delta T, \quad S(z=0) = S_0 + \Delta S, \quad T(z=d) = T_0, \quad S(z=d) = S_0. \tag{3.17}$$

Consider a region of volume V with boundary S' and outward normal $\mathbf{n}$. Mass is not created nor destroyed, the resulting mass equation for compressible fluids is given by

$$\frac{\partial \rho}{\partial t} + \underline{\nabla}.(\rho \mathbf{v}) = 0. \tag{3.18}$$

The conservation of mass equation for an incompressible fluids is,

$$\underline{\nabla} \cdot \mathbf{v} = 0, \tag{3.19}$$

since the density ρ is constant.

3.2.1 Momentum balance equation

The momentum balance equation is derived from Cauchy's first law of motion. Stress is force per unit area. Let $\mathbf{t}(\mathbf{n})$ be the stress exerted on the surface of an element by the fluid on the side to which $\mathbf{n}$ is directed. Where $\mathbf{t}(\mathbf{n})$ is the stress vector. Cauchy's formula

$$t_i(\mathbf{n}) = n_k \tau_{ki}, \tag{3.20}$$

gives the stress vector $\mathbf{t}(\mathbf{n})$ on a surface with arbitrary unit normal $\mathbf{n}$ in terms of the nine components of the stress tensor (3.5). Cauchy derived his first law of motion from the principle of linear momentum, which states that the rate of change of linear momentum of an arbitrary part P of the fluid equals the resultant force on P. Now consider a material volume V with surface S' consisting at all times of the same fluid particles and moving with the fluid. The i^{th} component of the force exerted by the surrounding fluid in V is given by

$$\int_{S'} t_i(\mathbf{n}) dS' = \int_{S'} n_k \tau_{ki} dS', \tag{3.21}$$

and therefore,

$$\int_{S'} t_i(\mathbf{n}) dS' = \int_V \tau_{ki,k} dV, \tag{3.22}$$

using the divergence theorem (3.1). Consider a small material volume δV, then $\tau_{ki,k}$ will be almost constant throughout δV. From the principle of linear momentum applied to δV, we have

$$\frac{D}{Dt}(\rho \delta V \ v_i) = \tau_{ki,k} \delta V + F_i \rho \delta V. \tag{3.23}$$

Since mass is conserved,

$$\frac{D}{Dt}(\rho \delta V) = 0, \tag{3.24}$$

and therefore,

$$\delta V \left(\rho \frac{Dv_i}{Dt} - \tau_{ki,k} - \rho F_i \right) = 0. \tag{3.25}$$

But, δV is arbitrary, thus

$$\rho \frac{Dv_i}{Dt} = \tau_{ki,k} + \rho F_i, \tag{3.26}$$

where F_i is the component of the body force per unit mass in the i^{th} direction. Equation (3.26) is known as Cauchy's first law of motion.

For a Newtonian fluid,

$$\tau_{ik} = (-p + \lambda\Gamma)\delta_{ik} + 2\mu D_{ik}, \tag{3.27}$$

where p is the pressure, λ is the coefficient of viscosity, μ is the dynamic viscosity, δ_{ik} is the unit stress tensor,

$$\delta_{ik} = \begin{cases} 1 & \text{if } i = k \\ 0 & \text{if } i \neq k. \end{cases} \tag{3.28}$$

μ is the coefficient of dynamic viscosity,

$$\Gamma = \underline{\nabla} \cdot \mathbf{v},$$

and D_{ik} is the rate of strain tensor,

$$D_{ik} = \frac{1}{2}\left(\frac{\partial v_i}{\partial x_k} + \frac{\partial v_k}{\partial x_i}\right).$$

For incompressible fluids, the density ρ is a constant.

$$\underline{\nabla} \cdot \mathbf{v} = 0.$$

Thus constitutive equation (3.27) reduces to

$$\tau_{ik} = -p\sigma_{ik} + 2\mu D_{ik}. \tag{3.29}$$

Substituting equation (3.29) into (3.26) we obtain

$$\rho\frac{D\mathbf{v}}{Dt} = -\underline{\nabla} p + \mu\nabla^2\mathbf{v} + \rho\mathbf{F}, \tag{3.30}$$

which is the Navier-Stokes equation for incompressible fluids.

Equation (3.30) is the momentum equation in an inertial frame of reference. The problem we are solving is in a rotating frame. We will utilize the rotating axis theorem to move from the inertial frame to a rotating frame.

3.2.2 The energy balance equation for the temperature

We use the energy balance equation to derive the temperature equation. Consider a material volume V with material surface S' containing of the same fluid particles moving with the fluid at all times. The repeated indices in our derivation imply summation. The first law of thermodynamics which is the energy balance equation states that the rate of change of kinetic energy in V plus the rate of change of internal energy in V is equal to the rate of heat flow into V plus the rate of work done by the surface stress $\mathbf{t}(\mathbf{n})$ plus the rate of work done by the body force $\mathbf{F}$.

For the rate of heat flow in V, let $\mathbf{H}$ be the heat flow vector, which satisfies Fourier's law of heat conduction (3.8)

$$\mathbf{H} = -\kappa \underline{\nabla} T, \tag{3.31}$$

where T is the temperature and κ is the coefficient of thermal conductivity. Let the rate of heat flow into V be denoted by h. Using the divergence theorem (3.1) we have

$$\begin{aligned} h &= -\int_{S'} \mathbf{H} \cdot \mathbf{n}\, dS' \\ &= -\int_{S'} (-\kappa) \underline{\nabla} T \cdot \mathbf{n}\, dS' \\ &= \kappa \int_V \nabla^2 T\, dV. \end{aligned} \tag{3.32}$$

Now consider a small volume δV. Then the rate of heat flow h into δV is

$$h = \kappa \nabla^2 T\, \delta V. \tag{3.33}$$

Let the rate of work done by surface stresses $\mathbf{t}(\mathbf{n})$ be denoted as q_{ss}, then q_{ss} is given by

$$q_{ss} = \int_{S'} \mathbf{t}(\mathbf{n}) \cdot \mathbf{v}\, dS' \tag{3.34}$$

$$= \int_{S'} n_k \tau_{ki} v_i\, dS', \tag{3.35}$$

where $\mathbf{v}$ is the velocity vector of the surface, and S' is the surface over which the work is being done. Using Cauchy's formulae and applying the divergence theorem (3.1), we obtain

$$q_{ss} = \int_V (\tau_{ki} v_i)_{,k}\ dV.$$

But

$$\tau_{ki} v_{ik} = \tau_{ik} D_{ik}.$$

since the Cauchy stress tensor is symmetric. Now consider an incompressible fluid, then

$$\tau_{ik} = -p\delta_{ik} + 2\mu D_{ik}, \tag{3.36}$$

where p is the pressure, $\delta_{ik} = 1$ for $i \neq k$ and 1 elsewhere, and D_{ik} are the strain components and $D_{ii} = \text{div}(\mathbf{v}) = 0$ from equation (3.19). Thus,

$$\tau_{ki} v_{i,k} = 2\mu D_{ik} D_{ik}, \tag{3.37}$$

and for small volume δV, the rate of work done by surface stresses $\mathbf{t}(\mathbf{n})$ is given by

$$q_{ss} = (\tau_{ki,k} v_i + 2\mu D_{ik} D_{ik})\delta V. \tag{3.38}$$

Let K_E and m denote the rate of change of kinetic energy and the mass associated with the volume of the fluid. For a small volume δV, q_{ss} is given by

$$q_{ss} = \frac{D}{Dt}\left(\frac{1}{2}\rho \delta V v_i v_i\right), \qquad (\rho \delta V = \delta m) \tag{3.39}$$

$$q_{ss} = v_i \rho \frac{Dv_i}{Dt} \delta V, \quad \left(\frac{D}{Dt} \rho \delta V = \frac{D}{Dt} \delta m = 0 \right). \tag{3.40}$$

Let I_E denote the rate of change of internal energy. For a small volume δV, I_E is given by

$$I_E = \frac{D}{Dt}(c_v T \rho \delta V) \tag{3.41}$$

$$I_E = c_v \rho \frac{DT}{Dt} \delta V, \quad \left(\frac{D}{Dt} \rho \delta V = \frac{D}{Dt} \delta m = 0 \right), \tag{3.42}$$

where T is the absolute temperature, c_v is the specific heat at constant volume. Now, let the work done by the body forces be denoted by q_{bf}. For a small volume δV, q_{bf} is given by

$$q_{bf} = \mathbf{F} \cdot \mathbf{v}, \tag{3.43}$$

$$q_{bf} = F_i v_i \delta V. \tag{3.44}$$

Therefore, substituting equations (3.33), (3.38), (3.40), (3.42), and (3.44) and simplifying we get the following

$$c_v \rho \frac{DT}{Dt} = \kappa \nabla^2 T + 2\mu D_{ik} D_{ik}. \tag{3.45}$$

The term $D_{ik}D_{ik}$ is the square of two terms. If D_{ik} is sufficiently small, then $D_{ik}D_{ik} \approx 0$. Therefore for sufficiently small D_{ik}, equation (3.45) simplifies to

$$\rho \frac{DT}{Dt} = \kappa_T \nabla^2 T, \tag{3.46}$$

where $\kappa_T = \kappa / c_v$ is the heat diffusion coefficient. Equation (3.46) is the temperature equation for incompressible fluids. Similarly, the salt equation is given by

$$\frac{DS}{Dt} = \kappa_S \nabla^2 S, \tag{3.47}$$

where κ_S is the salinity diffusion coefficient. In summary, equations (3.18), (3.30), (3.46), and (3.47) are the governing equations for double-diffusive convection in the inertial frame of reference.

3.3 Summary of equations in the inertial reference frame

Here, we summarize the essential equations of motion in an inertial reference frame. Momentum equation:

$$\rho \frac{D\mathbf{v}}{Dt} = -\underline{\nabla} p + \mu \nabla^2 \mathbf{v} + \rho \mathbf{F}. \tag{3.48}$$

Mass equation:

$$\underline{\nabla} \cdot \mathbf{v} = 0. \tag{3.49}$$

Temperature equation:

$$\rho \frac{DT}{Dt} = \kappa_T \nabla^2 T. \tag{3.50}$$

Salt equation:

$$\frac{DS}{Dt} = \kappa_S \nabla^2 S, \tag{3.51}$$

In the next section, we shall use the rotating axis theorem to shift from the inertial frame to the rotating frame.

3.4 Governing equations in a rotating frame

Consider the position vector $\mathbf{r}$,

$$\mathbf{r} = x\mathbf{i} + y\mathbf{j} + (z+a)\mathbf{k}$$

of a particle/object at the surface of the earth, where a is the radius of the Earth, θ is the angle measured from the horizontal plane to the position and $\mathbf{\Omega}$ is the angular velocity of the Earth. See Figure 3.2.

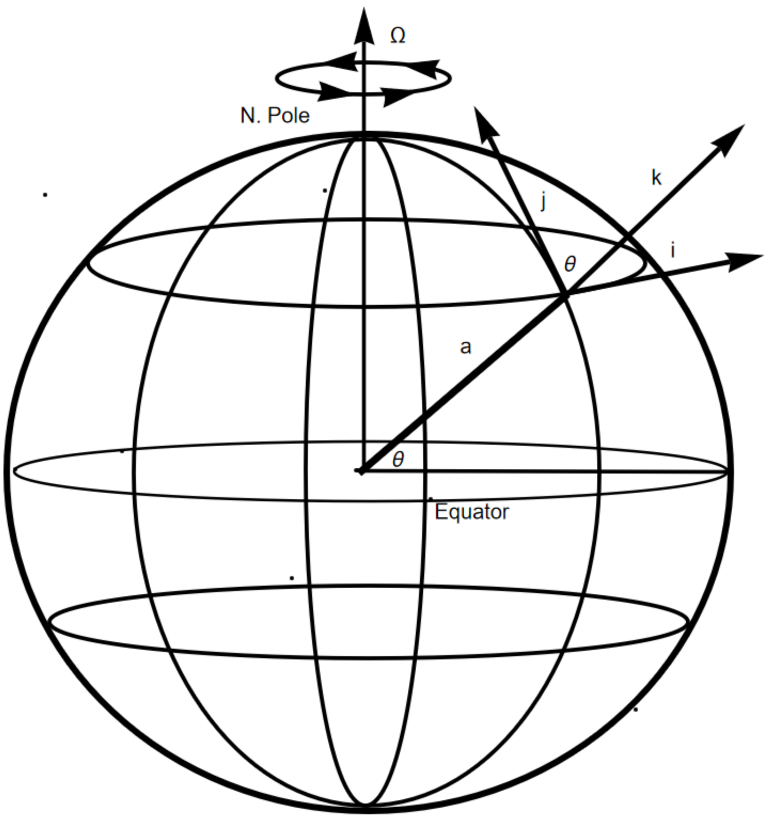

Figure 3.2: *Position of a body at the surface of the earth.*

3.4.1 Rotating axis theorem

Let $\mathbf{i}'$, $\mathbf{j}'$, $\mathbf{k}'$ be a rectangular reference fixed in space with origin O. Denote this frame by s_I. Let $\mathbf{i}$, $\mathbf{j}$, $\mathbf{k}$ be a rectangular frame rotating with angular velocity $\mathbf{\Omega}$. Let $\mathbf{f}$ be a position vector in a rotating system. Thus,

$$\mathbf{f} = f_1\mathbf{i} + f_2\mathbf{j} + f_3\mathbf{k}, \tag{3.52}$$

and

$$\mathbf{f} = f_1'\mathbf{i}' + f_2'\mathbf{j}' + f_3'\mathbf{k}', \tag{3.53}$$

that is

$$f_1\mathbf{i} + f_2\mathbf{j} + f_3\mathbf{k} = f_1'\mathbf{i}' + f_2'\mathbf{j}' + f_3'\mathbf{k}'. \tag{3.54}$$

Then the time rate of change concerning $\mathbf{f}$ is given by

$$\left(\frac{d\mathbf{f}}{dt}\right)_I = \frac{d(f_1'\,\mathbf{i}')}{dt} + \frac{d(f_2'\,\mathbf{j}')}{dt} + \frac{d(f_3'\,\mathbf{k}')}{dt}, \tag{3.55}$$

and

$$\left(\frac{d\mathbf{f}}{dt}\right)_R = \frac{d(f_1\,\mathbf{i})}{dt} + \frac{d(f_2\,\mathbf{j})}{dt} + \frac{d(f_3\,\mathbf{k})}{dt}, \tag{3.56}$$

subscript I and subscript R denote the inertial and rotating frames, respectively. Equation (3.56) reduces to

$$\left(\frac{d\mathbf{f}}{dt}\right)_R = \frac{df_1}{dt}\mathbf{i} + \frac{df_2}{dt}\mathbf{j} + \frac{df_3}{dt}\mathbf{k}, \tag{3.57}$$

and equation (3.55) reduces to

$$\begin{aligned}
\left(\frac{d\mathbf{f}}{dt}\right)_I &= \frac{df_1'}{dt}\mathbf{i}' + \frac{df_2'}{dt}\mathbf{j}' + \frac{df_3'}{dt}\mathbf{k}' + f_1'\frac{d\mathbf{i}'}{dt} + f_2'\frac{d\mathbf{j}'}{dt} + f_3'\frac{d\mathbf{k}'}{dt} \\
&= \frac{df_1'}{dt}\mathbf{i}' + \frac{df_2'}{dt}\mathbf{j}' + \frac{df_3'}{dt}\mathbf{k}' + f_1'(\boldsymbol{\Omega}\times\mathbf{i}') + f_2'(\boldsymbol{\Omega}\times\mathbf{j}') + f_3'(\boldsymbol{\Omega}\times\mathbf{k}') \\
&= \frac{df_1'}{dt}\mathbf{i}' + \frac{df_2'}{dt}\mathbf{j}' + \frac{df_3'}{dt} + \boldsymbol{\Omega}\times\mathbf{f}.
\end{aligned} \tag{3.58}$$

For any vector $\mathbf{v}$,

$$\left(\frac{d\mathbf{v}}{dt}\right)_R = \left(\frac{d\mathbf{v}}{dt}\right)_I + \boldsymbol{\Omega}\times\mathbf{v},$$

in a rotating frame and

$$\left(\frac{d\mathbf{v}}{dt}\right)_I = 0,$$

in the inertial frame. Thus using equation (3.57), (3.58), and (3.54) we obtain the following

$$\left(\frac{d\mathbf{f}}{dt}\right)_I = \left(\frac{d\mathbf{f}}{dt}\right)_R + \boldsymbol{\Omega}\times\mathbf{f}, \tag{3.59}$$

where $\boldsymbol{\Omega} = (\Omega_x, \Omega_y, \Omega_z)$ is the angular velocity vector. Equation (3.59) is known as the rotating axis theorem.

3.4.2 The momentum equation in the rotating frame

Let

$$\mathbf{r} = x(t)\mathbf{i} + y(t)\mathbf{j} + (z(t) + a)\mathbf{k}$$

be the position vector on the surface of the Earth, where a is the radius of the Earth, and

$$\boldsymbol{\Omega} = (0, \Omega_y, \Omega_z) = (0, \Omega\cos\theta, \Omega\sin\theta) \tag{3.60}$$

be the angular velocity of the system. The angle θ is measured from the line of latitude (equator) to the line of longitude. Then applying equation (3.59) we get the following

$$\left(\frac{d\mathbf{r}}{dt}\right)_I = \left(\frac{d\mathbf{r}}{dt}\right)_R + \boldsymbol{\Omega} \times \mathbf{r}, \tag{3.61}$$

or,

$$\mathbf{v}_I = \mathbf{v_R} + \boldsymbol{\Omega} \times \mathbf{r}, \tag{3.62}$$

where $\mathbf{v}_I$ and $\mathbf{v}_R$ are the velocity vectors in the inertial and rotating frames, respectively. Applying $\mathbf{v}_I$ on theorem (3.59) to obtain the acceleration yields the following,

$$\begin{aligned}\left(\frac{d\mathbf{v}_I}{dt}\right)_I &= \left(\frac{d\mathbf{v}_I}{dt}\right)_R + \boldsymbol{\Omega} \times \mathbf{v}_I \\ &= \left(\frac{d(\mathbf{v_R} + \boldsymbol{\Omega} \times \mathbf{r})}{dt}\right)_I + \boldsymbol{\Omega} \times (\mathbf{v_R} + \boldsymbol{\Omega} \times \mathbf{r}).\end{aligned} \tag{3.63}$$

Since $\boldsymbol{\Omega}$ is a constant, the above equation can be reduced to,

$$\left(\frac{d\mathbf{v}_I}{dt}\right)_I = \left(\frac{d\mathbf{v}_R}{dt}\right)_R + 2\boldsymbol{\Omega} \times \mathbf{v}_R + \boldsymbol{\Omega} \times (\boldsymbol{\Omega} \times \mathbf{r}), \tag{3.64}$$

where $2\boldsymbol{\Omega} \times \mathbf{v}_R$ is due to the Coriolis effect force, while $\boldsymbol{\Omega} \times (\boldsymbol{\Omega} \times \mathbf{r})$ is a consequence of the centrifugal force effect, and $d\mathbf{v}/dt$ is the acceleration of the fluid particle. Consider the viscous term of the momentum equation ($\mu\nabla^2\mathbf{v}_I$). Substituting

$$\mathbf{v}_I = \mathbf{v_R} + \boldsymbol{\Omega} \times \mathbf{r}$$

into the viscous term gives,

$$\mu\nabla^2\mathbf{v}_I = \mu\nabla^2(\mathbf{v}_R + \boldsymbol{\Omega} \times \mathbf{r}), \tag{3.65}$$

which simplifies to,

$$\mu\nabla^2\mathbf{v}_I = \mu\nabla^2\mathbf{v}_R, \tag{3.66}$$

since

$$(\boldsymbol{\Omega} \times \mathbf{r}) = \Omega\left((z+a)\cos\theta - y\sin\theta\right)\ \mathbf{i} + \Omega(x\sin\theta)\ \mathbf{j} - \Omega(x\cos\theta)\ \mathbf{k},$$

therefore

$$\nabla^2(\boldsymbol{\Omega} \times \mathbf{r}) = 0.$$

Because,

$$\nabla^2 = \frac{\partial^2}{\partial x^2} + \frac{\partial^2}{\partial y^2} + \frac{\partial^2}{\partial z^2},$$

and

$$\mathbf{\Omega} \times \mathbf{r},$$

depends only on x, y, z. Substituting equation (3.65) and (3.63) into equation (3.30) and rearranging we get

$$\rho\frac{\partial \mathbf{q}}{\partial t} + (\mathbf{q}\cdot\underline{\nabla})\mathbf{q} = -\underline{\nabla} p - \rho g(t)\mathbf{k} + \mu\nabla^2\mathbf{q} - 2\rho\mathbf{\Omega}\times\mathbf{q} - \rho\mathbf{\Omega}\times(\mathbf{\Omega}\times\mathbf{r}), \tag{3.67}$$

where

$$\mathbf{q} = \mathbf{v}_R = (u, v, w)$$

is the velocity vector in the rotating frame, p is the pressure, g is the gravitational acceleration, $\mathbf{k}$ is a base vector in the z direction, and ν is the kinematic viscosity. Equation (3.67) is the momentum equation in a rotating frame. We can rewrite the last term of the equation (3.67) as a divergence of a scalar potential [53]. That is,

$$\mathbf{F}_{ce} = \rho\mathbf{\Omega}\times(\mathbf{\Omega}\times\mathbf{r}) = -\rho\underline{\nabla}\Phi_{ce}, \tag{3.68}$$

where

$$\Phi_{ce} = (\Omega\times\mathbf{r})^2/2.$$

Combining the pressure term and $\mathbf{F}_{ce}$ we obtain,

$$\nabla P = -\underline{\nabla}\left(\frac{p}{\rho} + \Phi_{ce}\right).$$

P is known as the hydrostatic pressure of the system, where

$$P = p + \rho\Phi_{ce}.$$

Therefore, equation (3.67) reduces to,

$$\rho\frac{\partial \mathbf{q}}{\partial t} + (\mathbf{q}\cdot\underline{\nabla})\mathbf{q} = -\underline{\nabla} P - \rho g(t)\mathbf{k} + \mu\nabla^2\mathbf{q} - 2\rho\mathbf{\Omega}\times\mathbf{q}, \tag{3.69}$$

where $\mathbf{k}$ is a base vector. Consider the mass equation (3.19). Substituting $\mathbf{v}_I = \mathbf{v}_R + (\mathbf{\Omega}\times\mathbf{r})$ into the mass equation yields,

$$\begin{aligned}\underline{\nabla}\cdot\mathbf{v}_I &= \underline{\nabla}\cdot(\mathbf{v_R} + (\mathbf{\Omega}\times\mathbf{r}))\\ &= \underline{\nabla}\cdot\mathbf{v}_R + \underline{\nabla}\cdot(\mathbf{\Omega}\times\mathbf{r}),\end{aligned} \tag{3.70}$$

but $\boldsymbol{\nabla}\cdot(\mathbf{\Omega}\times\mathbf{r}) = 0$ since $(\mathbf{\Omega}\times\mathbf{r})$ is a constant vector. Therefore,

$$\underline{\nabla}\cdot\mathbf{v}_I = \underline{\nabla}\cdot\mathbf{v}_R. \tag{3.71}$$

For scalar-valued functions, the rotation has no effect. Thus, the temperature and salt equations remain unchanged/unaffected in the process [53].

3.5 Equations of motion in a rotating frame

We apply the rotating axis theorem to transition from the inertial frame of reference to the rotating frame of reference. In the rotating frame, two fictitious forces arise, the Coriolis force and the centrifugal force. The centrifugal force is absorbed in the pressure term whereas the Coriolis force is to play an active role. We further introduce a sinusoidal time-dependent gravity modulation. The mass equation and the marginal departure remain invariant in the rotating frame. Furthermore, the transition from inertial to a rotating frame leaves the temperature and salt equations unchanged. Thus equation (3.18) is identically satisfied. Therefore, the governing equations for double-diffusive convection in rotating incompressible fluids are.
Momentum:

$$\rho\frac{\partial \mathbf{q}}{\partial t} + (\mathbf{q}\cdot\underline{\nabla})\mathbf{q} = -\underline{\nabla}P - \rho g(t)\mathbf{k} + \mu\nabla^2\mathbf{q} - 2\rho\mathbf{\Omega}\times\mathbf{q}. \tag{3.72}$$

Continuity equation:

$$\underline{\nabla}\cdot\mathbf{q} = 0, \tag{3.73}$$

Temperature gradient:

$$\frac{\partial T}{\partial t} + (\mathbf{q}\cdot\underline{\nabla})\,T = \kappa_T\nabla^2 T, \tag{3.74}$$

Salinity gradient:

$$\frac{\partial S}{\partial t} + (\mathbf{q}\cdot\underline{\nabla})\,S = \kappa_S\nabla^2 S, \tag{3.75}$$

where $\mathbf{q} = (u, v, w)$ is the velocity vector, P is the system's static pressure, $g(t)$ is the time-dependent gravitational acceleration, and ω is the modulation frequency. The parameter μ is the dynamic viscosity, Ω is the angular velocity of the system, and $\mathbf{k}$ is the direction vector. The parameters, T and S, are the temperature and salinity, respectively. The parameters κ_T and κ_S are diffusivity constant for heat and salt, respectively. The terms $\frac{\partial \mathbf{q}}{\partial t} + (\mathbf{q}\cdot\underline{\nabla})\mathbf{q}$ are the inertial forces, ∇P are the pressure gradient forces, $\rho g(t)$ is the buoyancy term, $\mu\nabla^2\mathbf{q}$ are the viscous terms, and $-2\rho\mathbf{\Omega}\times\mathbf{q}$ is the Coriolis force.

Equations (3.72) to (3.75) describe fluid dynamics in the ocean, particularly focusing on convection processes. However, these are incomplete without the equation of state The ocean's high salinity level (ranging from 33 to 37 grams per liter) affects the density of ocean water. Temperature and salinity gradients create vertical density variations, leading to ocean water instability. Notably, temperature diffuses much faster than salt in water, making many ocean regions prone to double-diffusive convection.

Temperature and salinity gradients have opposing effects on water density. A positive temperature gradient increases fluid molecule kinetic energy, causing expansion and decreased density. Conversely, a positive salinity gradient reduces fluid kinetic energy, increasing density. Therefore, the combined influence of temperature and salinity changes governs the system's density.

The changes in density depend on how much the water contracts or expands. Mathematically, the following equation describes the effect of contraction or expansion of water in the ocean during double-diffusive convection. If there are density variations (denoted ρ_1) and

$$\rho = \rho_0 + \rho_1,$$

then we can calculate an expression for ρ_1 where

$$T = T_0 + T_1,$$

and

$$S = S_0 + S_1,$$

where T_0 and S_0 are the initial temperature and salt, and ρ_0 is the initial density of the system corresponding to T_0 and S_0. We can expand $\rho(T, S)$ using the Taylor series expansion around T_0 and S_0 to obtain,

$$\begin{aligned}\rho(S,T) &= \rho\left[T_0 + (T - T_0),\ S_0 + (S - S_0)\right] \\ &= \rho(T_0, S_0) + \frac{\partial \rho(T_0, S_0)}{\partial T}(T - T_0) \\ &+ \frac{\partial \rho(T_0, S_0)}{\partial S}(S - S_0) + O((T - T_0)^2 + (S - S_0)^2).\end{aligned} \tag{3.76}$$

Now we have,

$$\begin{aligned}\rho &= \rho(T_0,\ S_0) + \rho_1(T, S) \\ &= \rho_0 + \rho_1(T, S).\end{aligned} \tag{3.77}$$

Thus, neglecting second-order terms in $(T - T_0)$ and $(S - S_0)$ in equation (3.76) we obtain the following,

$$\rho_0 + \rho_1(T, S) \approx \rho(T_0, S_0) + \frac{\partial \rho(T_0, S_0)}{\partial T}(T - T_0) + \frac{\partial \rho(T_0, S_0)}{\partial S}(S - S_0). \tag{3.78}$$

Hence,

$$\rho_1(T, S) \approx \frac{\partial \rho(T_0, S_0)}{\partial T}(T - T_0) + \frac{\partial \rho(T_0, S_0)}{\partial S}(S - S_0). \tag{3.79}$$

We define the following,

$$\alpha = -\frac{1}{\rho(T_0, S_0)}\frac{\partial \rho}{\partial T} \qquad \text{and} \qquad \beta = \frac{1}{\rho(T_0, S_0)}\frac{\partial \rho}{\partial S}, \tag{3.80}$$

where α is the coefficient of thermal expansion of the fluid and β is the coefficient of fluid contraction. Consider a fluid element of volume V and mass m, consisting at all times of the same fluid particles. The salt content remains constant. Then m remains constant. Now, by definition,

$$\rho = \frac{m}{V}.$$

Thus,

$$\alpha = -\frac{1}{\rho}\frac{\partial \rho}{\partial T} = -\frac{V}{m}\frac{\partial}{\partial T}\left(\frac{m}{V}\right). \tag{3.81}$$

Differentiating we obtain the following,

$$\alpha = \frac{1}{v}\frac{\partial V}{\partial T}. \tag{3.82}$$

Now, consider a fluid element of volume V and mass m, consisting at all times of the same fluid particles. The temperature remains constant, but the salt content changes. In this case, the volume remains constant while the mass changes. Thus,

$$\beta = \frac{1}{\rho}\frac{\partial \rho}{\partial S} = -\frac{V}{m}\frac{\partial}{\partial S}\left(\frac{m}{V}\right). \tag{3.83}$$

Simplifying and differentiating we obtain,

$$\beta = \frac{1}{m}\frac{\partial m}{\partial S}. \tag{3.84}$$

Therefore, α denotes the change in volume per unit volume per temperature rise, and β denotes the change in mass per unit mass per rise in salinity. From equation (3.80),

$$\frac{\partial \rho(T_0, S_0)}{\partial T} = -\rho(T_0, S_0)\alpha(T_0, S_0), \qquad \frac{\partial \rho(T_0, S_0)}{\partial S} = \rho(T_0, S_0)\beta(T_0, S_0). \tag{3.85}$$

Let,

$$\rho_0 = \rho(T_0, S_0), \qquad \alpha_0 = \alpha(T_0, S_0), \qquad \text{and} \qquad \beta_0 = \beta(T_0, S_0),$$

then,

$$\frac{\partial \rho}{\partial T}(T_0, S_0) = -\rho_0\alpha_0, \qquad \text{and} \qquad \frac{\partial \rho}{\partial S}(T_0, S_0) = \rho_0\beta_0. \tag{3.86}$$

From equation (3.79),

$$\rho_1(T, S) = \rho_0[-\alpha_0(T - T_0) + \beta_0(S - S_0)], \tag{3.87}$$

where

$$T = T_0 + T_1, \quad \text{and} \quad S = S_0 + S_1,$$

for $\alpha_0 > 0$ and $\beta_0 > 0$. Equation (3.87) is known as *the equation of state* for double-diffusive convection.

The oceans are significant in regulating climate change, feeding, and generating most of the oxygen we breath. Their significance is mainly due to the convection and ocean circulation processes that take place. The study of convection in the ocean is well-known in oceanography. Recently, the effects of gravity variations on the ocean bottom have drawn much attention from researchers. These variations are primarily due to pressure differences and the rapid shifting of mass in the ocean. The pressure differences are largely due to glaciers melting, waste products from human activity, and the movement of tectonic plates.

We know gravity pulls stronger on dense objects than on lighter ones. This property of gravity gives rise to different areas of the ocean experiencing varying gravitational pull due to pressure differences in the ocean bottom. Although these variations in gravity are minor ($\pm 10^{-3}\ m/s^2$), the National Aeronautics and Space Administration (NASA) showed that their effect on circulation is significant in large-scale problems. This variation in gravity is known as gravity modulation, an essential component of convection analysis. The fluid moves up and down sinusoidally during a double-diffusive convection process. Thus, we will use a time-dependent sine-like function to track the variations in gravity. This function relates the initial gravity g_0 to the changes in gravity using the frequency and amplitude of modulation. That is,

$$g_m(t) = g_0 \left[1 + \delta \sin\left(\omega_m t\right)\right], \tag{3.88}$$

where δ is the modulation amplitude, ω_g is the frequency of modulation, and $g = g_m(t)$ is the modulated gravity. Equations (3.72)-(3.88) are the governing equations for double-diffusive convection in a rotating frame with gravity modulation.

3.6 Summary

In this chapter, we have derived the equations of motion governing double-diffusive convection in an inertial reference frame. Since we are considering application in the ocean, where rotation cannot be ignored, we applied the rotating axes theorem to transition from inertial to rotating reference frame.

Chapter 4

Linear Stability Analysis

4.1 Introduction

In this chapter, we conduct linear stability analysis on the set of equations of motion derived in Chapter 3. We first employ dimensional analysis on the equations and apply the Boussinesq approximation, which assumes the density of the fluid to be constant in all terms of the momentum equation except in the buoyancy term. We then conduct both stationary and oscillatory convection using normal modes. Consider the following model of the double-diffusive convection process between two horizontal layers heated from below. We refer the reader to Figure (3.1) which is a layer of fluid confined between two horizontal layers, undergoing natural convection driven by temperature and salt subject to heating from below.

4.2 The background state equations

The governing equations (3.72) - (3.75) when velocity in the background state $\mathbf{q}_b = (0, 0, 0)$, and assumed to be independent of time reduce to,

$$\frac{\partial P_b}{\partial x} = 0, \tag{4.1}$$

$$\frac{\partial P_b}{\partial y} = 0, \tag{4.2}$$

$$\frac{\partial P_b}{\partial z} = -\rho g_m(t), \tag{4.3}$$

where the subscript $'b'$ refers to the background state and g_m refers to modulated gravity. But equations (4.1) and (4.2) indicates that $P_b = P_b(z)$, thus

$$\frac{dP_b(z)}{dz} = -\rho g_m(t), \tag{4.4}$$

$$\frac{d^2T_b(z)}{dz^2} = 0, \quad \text{and} \quad \frac{d^2S_b(z)}{dz^2} = 0, \tag{4.5}$$

subject to the following boundary conditions,

$$\begin{aligned} T_b(0) &= T_0 + \Delta T, \quad T_b(d) = T_0, \\ S_b(0) &= S_0 + \Delta S, \quad S_b(d) = S_0. \end{aligned} \tag{4.6}$$

Equations (4.5) are solved for $T_b(z)$ and $S_b(z)$ to obtain,

$$T_b(z) = T_0 + \Delta T \left(1 - \frac{z}{d}\right), \tag{4.7}$$

$$S_b(z) = S_0 + \Delta S \left(1 - \frac{z}{d}\right), \tag{4.8}$$

where $P_b(z)$, $T_b(z)$, and $S_b(z)$ are the background pressure, temperature, and salinity respectively.

4.3 Dimensional Analysis

We now consider dimensional analysis on equations (3.72),(3.73),(3.74) and (3.87). Moving from the background state, we will get perturbations of the following nature:

$$T(t, x, y, z) = T_b(z) + T'(t, x, y, z), \tag{4.9}$$

$$S(t, x, y, z) = S_b(z) + S'(t, x, y, z) \tag{4.10}$$

$$\rho(t, x, y, z) = \rho_b(z) + \rho'(t, x, y, z). \tag{4.11}$$

From equation (3.87),

$$\rho' = \rho_b[-\alpha(T_b, S_b)T' + \beta(T_b, S_b)S']. \tag{4.12}$$

$$g_m(t) = g_0 \left[1 + \delta \sin(\omega_m t)\right], \tag{4.13}$$

$$P(t, x, y, z) = P_b(z) + P'(t, x, y, z). \tag{4.14}$$

$$\mathbf{q}(t, x, y, z) = \mathbf{q_b} + \mathbf{q}'(t, x, y, z), \tag{4.15}$$

where T', S', P' and $\mathbf{q}'$ are the perturbations. Since $\mathbf{q_b} = \underline{\mathbf{0}}$, substituting equation (4.9) into equation (3.74) we obtain the following equations

$$\begin{aligned} \frac{D(T_b + T')}{Dt} &= \frac{DT'}{Dt} + \frac{DT_b}{Dt} \\ &= \frac{\partial T'}{\partial t} + (\mathbf{q}' \cdot \underline{\nabla})\, T' + \frac{\partial T_b}{\partial t} + (\mathbf{q}' \cdot \underline{\nabla})\, T_b \\ &= \frac{\partial T'}{\partial t} + (\mathbf{q}' \cdot \underline{\nabla})\, T' + w\frac{dT_b}{dz}. \end{aligned}$$

Therefore,

$$\frac{\partial T'}{\partial t} + (\mathbf{q}' \cdot \underline{\nabla})\, T' - w\frac{\Delta T}{d} = \kappa_T \nabla^2 T'. \tag{4.16}$$

Similarly, substituting equation (4.10) into equation (3.75) we obtain

$$\frac{\partial S'}{\partial t} + (\mathbf{q}' \cdot \underline{\nabla})\, S' - w\frac{\Delta S}{d} = \kappa_S \nabla^2 S'. \tag{4.17}$$

In the next Sub-section, we will use the Boussinesq approximation to consider the perturbed momentum equation.

4.3.1 Boussinesq approximation

We apply the Boussinesq approximation for the perturbations of the equation (3.72). The Boussinesq approximation is a simplification used in fluid dynamics, particularly for buoyancy-driven flows like natural convection. This approximation is most effective when dealing with incompressible fluids experiencing small temperature variations. It helps with complex fluid dynamic equations, making them more manageable for certain types of analysis.

At its core, the Boussinesq approximation assumes that the fluid's density remains constant throughout the flow, except when it comes to the buoyancy term in the Navier-Stokes equations. This means that density variations are only taken into account when they influence the buoyancy force, which drives the motion of the fluid.

A key aspect of this approximation is the treatment of the fluid as incompressible. This assumption simplifies the continuity equation, which governs the conservation of mass, to a more manageable form. Because of these simplifications, the Boussinesq approximation is particularly useful in studying natural convection, where fluid movement is primarily driven by temperature differences, and in fields like oceanography and atmospheric science, where large-scale flows often involve small temperature variations.

However, the Boussinesq approximation has its limitations. It is only valid when temperature variations are small enough that the resulting density changes are negligible. In situations where temperature differences are large, this approximation may no longer hold, and a more complex, fully compressible model would be necessary to describe the fluid's behavior accurately. Here, the density is substituted with a reference density value, usually representing the fluid's density at a specific temperature and salinity.

Substituting equations (4.9-4.15) into equation (3.72) we obtain the following,

$$\begin{aligned}(\rho_b+\rho')\left[\frac{\partial \mathbf{q}'}{\partial t}+(\mathbf{q}'\cdot\underline{\nabla})\mathbf{q}'\right] &= -\underline{\nabla}(P_b+P')+\mu\nabla^2\mathbf{q}'-(\rho_b+\rho')g_0(1+\delta\sin\omega_m t)\mathbf{k} \\ &- 2(\rho_b+\rho')\mathbf{\Omega}\times\mathbf{q}'. \end{aligned} \tag{4.18}$$

But for the background state,

$$0=-\underline{\nabla}P_b-\rho_b g_0(1+\delta\sin\omega_m t). \tag{4.19}$$

Hence,

$$\begin{aligned}(\rho_b+\rho')\left[\frac{\partial \mathbf{q}'}{\partial t}+(\mathbf{q}'\cdot\underline{\nabla})\mathbf{q}'\right] &= -\underline{\nabla}P'+\mu\nabla^2\mathbf{q}'-\rho' g_0(1+\delta\sin\omega_m t)\mathbf{k} \\ &- 2(\rho_b+\rho')\mathbf{\Omega}\times\mathbf{q}'. \end{aligned} \tag{4.20}$$

Divide by $\rho_b+\rho'$,

$$\begin{aligned}\left[\frac{\partial \mathbf{q}'}{\partial t}+(\mathbf{q}'\cdot\underline{\nabla})\mathbf{q}'\right] &= -\frac{1}{\rho_b+\rho'}\underline{\nabla}P'+\frac{\mu}{\rho_b+\rho'}\nabla^2\mathbf{q}' \\ &- \frac{\rho'}{\rho_b+\rho'}g_0(1+\delta\sin\omega_m t)\mathbf{k}-\frac{\rho_b+\rho'}{\rho_b+\rho'}2\mathbf{\Omega}\times\mathbf{q}'. \end{aligned} \tag{4.21}$$

We now make the Boussinesq approximation,

$$\begin{aligned} \frac{1}{\rho_b+\rho'}\underline{\nabla}P' &\approx \frac{1}{\rho_b}\underline{\nabla}P' \\ &\approx \frac{1}{\rho_0}\underline{\nabla}P', \end{aligned} \tag{4.22}$$

$$\begin{aligned} \frac{\mu}{\rho_b+\rho'} &\approx \frac{\mu}{\rho_b} \\ &\approx \frac{\mu}{\rho_0} \\ &= \nu. \end{aligned} \tag{4.23}$$

$$\begin{aligned} \frac{\rho'}{\rho_b+\rho'} &\approx \frac{\rho_b}{\rho_b}(-\alpha(T_b,S_b)T'+\beta(T_b,S_b)S') \\ &= (-\alpha(T_b,S_b)T'+\beta(T_b,S_b)S'). \end{aligned} \tag{4.24}$$

Using equation(4.23)-(4.25) the momentum equation reduces to,

$$\frac{\partial \mathbf{q}'}{\partial t}+(\mathbf{q}'\cdot\underline{\nabla})\mathbf{q}' = -\frac{1}{\rho_0}\underline{\nabla}\,P'+(\alpha T'-\beta S')\,g_0(1+\delta\sin\omega_m t)\,\mathbf{k}+\nu\nabla^2\mathbf{q}'-2\boldsymbol{\Omega}\times\mathbf{q}'. \tag{4.25}$$

Equations (4.16)-(4.25), (4.11) and (4.13) are the resulting perturbation equations for the system. We use the following non-dimensional variable

$$(x^*,y^*,z^*)=\frac{1}{d}(x,y,z),\quad (u^*,v^*,w^*)=\frac{d}{\kappa_T}(u',v',w'),$$

$$t^*=t\frac{\kappa_T}{d^2},\qquad S^*=\frac{S'}{\Delta S},\quad P^*=P'\frac{d^2}{\kappa_T\mu}\ \text{ and }\ T^*=\frac{T'}{\Delta T},$$

to non-dimensionalize our perturbation system. Dropping the asterisks for clarity and applying the Boussinesq approximation, which assumes that the variation in density only affects the buoyancy term and not the entire flow field, we obtain the following. Therefore, equations (3.72)-(3.75) become,

$$\underline{\nabla}\cdot\mathbf{q}=0, \tag{4.26}$$

$$\begin{aligned} \frac{1}{Pr}\left[\frac{\partial\mathbf{q}}{\partial t}+(\mathbf{q}\cdot\underline{\nabla})\mathbf{q}\right] &= -\underline{\nabla}P+\nabla^2\mathbf{q}+(R_TT-R_SS)(1+\delta\sin\omega_m t)\mathbf{k} \\ &\quad -\sqrt{Ta}(\cos\theta\mathbf{j}+\sin\theta\mathbf{k})\times\mathbf{q}, \end{aligned} \tag{4.27}$$

$$\frac{\partial T}{\partial t}+(\mathbf{q}\cdot\underline{\nabla})T-w=\nabla^2T, \tag{4.28}$$

$$\frac{\partial S}{\partial t}+(\mathbf{q}\cdot\underline{\nabla})S-w=Le^{-1}\nabla^2S, \tag{4.29}$$

where,

$$R_T=\frac{g_0\alpha\Delta Td^3}{\nu\kappa_T},\quad R_S=\frac{g_0\beta\Delta Sd^3}{\nu\kappa_S},\quad Pr=\frac{\nu}{\kappa_T},\quad Ta=\frac{4d^4\Omega^2}{\nu^2},$$

where R_T is the thermal Rayleigh number, R_S is the salinity Rayleigh number, Pr is the Prandtl number, and Ta is the Taylor number.

4.4 Normal mode analysis

In this section, we will conduct a linear stability analysis utilizing the method of normal modes. We will focus on the $z-$ component of our system as instability within the system is predominantly influenced by vertical motion. We first take the curl of equation (4.27) to eliminate the pressure term in our problem. Define

$$\begin{aligned}\boldsymbol{\zeta} &= \underline{\nabla} \times \mathbf{q}, \\ &= (\zeta_x, \zeta_y, \zeta_z),\end{aligned}$$

and

$$g_1(t) = 1 + \delta \sin \omega_m t.$$

Then

$$\begin{aligned}\underline{\nabla} \times \left[\frac{1}{Pr}\left(\frac{\partial \mathbf{q}}{\partial t} + (\mathbf{q} \cdot \underline{\nabla})\mathbf{q}\right)\right] &= \underline{\nabla} \times \left[-\underline{\nabla} P + \nabla^2 \mathbf{q} + (R_T T - R_S S) g_1(t) \mathbf{k}\right] \\ &\underline{\nabla} \times \left[-\sqrt{Ta}(\cos\theta \mathbf{j} + \sin\theta \mathbf{k}) \times \mathbf{q}\right].\end{aligned} \tag{4.30}$$

The simplifications of the terms in equation (4.30) are given by:

$$\underline{\nabla} \times \left[\frac{1}{Pr}\frac{\partial \mathbf{q}}{\partial t}\right] = \frac{1}{Pr}\frac{\partial \boldsymbol{\zeta}}{\partial t}, \tag{4.31}$$

$$\underline{\nabla} \times \left[\frac{1}{Pr}(\mathbf{q} \cdot \underline{\nabla})\mathbf{q}\right] = \frac{1}{Pr}\left[(\mathbf{q} \cdot \underline{\nabla})\boldsymbol{\zeta} - (\boldsymbol{\zeta} \cdot \underline{\nabla})\mathbf{q}\right]. \tag{4.32}$$

We neglect the second-order terms of equation (4.32).

$$\underline{\nabla} \times (\underline{\nabla} P) = \underline{\mathbf{0}}, \tag{4.33}$$

$$\underline{\nabla} \times (\nabla^2 \mathbf{q}) = \nabla^2 \boldsymbol{\zeta}, \tag{4.34}$$

$$\begin{aligned}\underline{\nabla} \times [(R_T T - R_S S) g_1(t)]\mathbf{k} &= \left(R_T \frac{\partial T}{\partial y} - R_S \frac{\partial S}{\partial y}\right) g_1(t)\mathbf{i} \\ &- \left(R_T \frac{\partial T}{\partial x} - R_S \frac{\partial S}{\partial x}\right) g_1(t)\mathbf{j},\end{aligned} \tag{4.35}$$

and

$$\underline{\nabla} \times \left[\sqrt{Ta}(\cos\theta \mathbf{j} + \sin\theta \mathbf{k}) \times \mathbf{q}\right] = -\sqrt{Ta}\left(\cos\theta \frac{\partial \mathbf{q}}{\partial y} + \sin\theta \frac{\partial \mathbf{q}}{\partial z}\right). \tag{4.36}$$

Substituting equations (4.31-4.36) into equation (4.30) we obtain,

$$\begin{aligned}\frac{1}{Pr}\left(\frac{\partial \boldsymbol{\zeta}}{\partial t}\right) &= \frac{\partial}{\partial y}(R_T T - R_S S) g_1(t)\mathbf{i} - \frac{\partial}{\partial x}(R_T T - R_S S) g_1(t)\mathbf{j} \\ &+ \nabla^2 \boldsymbol{\zeta} + \sqrt{Ta}\left(\sin\theta \frac{\partial \mathbf{q}}{\partial z} + \cos\theta \frac{\partial \mathbf{q}}{\partial y}\right).\end{aligned} \tag{4.37}$$

We further take the curl of (4.37) to obtain the vorticity transport equation. Doing so allows us to have a system of four equations and four unknowns.

$$
\begin{aligned}
\underline{\nabla} \times \left[\frac{1}{Pr}\left(\frac{\partial \boldsymbol{\zeta}}{\partial t}\right)\right] &= \underline{\nabla} \times \left[\frac{\partial}{\partial y}(R_T T - R_S S)g_1(t)\mathbf{i} - \frac{\partial}{\partial x}(R_T T - R_S S)g_1(t)\mathbf{j}\right] \\
&+ \underline{\nabla} \times \left[\nabla^2 \boldsymbol{\zeta} + \sqrt{Ta}\left(\sin\theta\frac{\partial \mathbf{q}}{\partial z} + \cos\theta\frac{\partial \mathbf{q}}{\partial y}\right)\right].
\end{aligned}
\tag{4.38}
$$

Each term of equation (4.38) when simplified gives,

$$
\underline{\nabla} \times \left[\frac{1}{Pr}\left(\frac{\partial \boldsymbol{\zeta}}{\partial t}\right)\right] = -\frac{1}{Pr}\left(\frac{\partial \nabla^2 \boldsymbol{q}}{\partial t}\right), \tag{4.39}
$$

$$
\underline{\nabla} \times \left(\nabla^2 \boldsymbol{\zeta}\right) = -\nabla^4 \mathbf{q}, \tag{4.40}
$$

$$
\begin{aligned}
&\underline{\nabla}\times \left[\frac{\partial}{\partial y}(R_T T - R_S S)g_1(t)\mathbf{i} - \underline{\nabla} \times \frac{\partial}{\partial x}(R_T T - R_S S)g_1(t)\mathbf{j}\right] \\
&= \left[\frac{\partial^2}{\partial z \partial x}(R_T T - R_S S)g_1(t)\right]\mathbf{i} + \left[\frac{\partial^2}{\partial y \partial z}(R_T T - R_S S)g_1(t)\right]\mathbf{j} \\
&- \left[\left(\frac{\partial^2}{\partial x^2} + \frac{\partial^2}{\partial y^2}\right)(R_T T - R_S S)g_1(t)\right]\mathbf{k},
\end{aligned}
\tag{4.41}
$$

$$
\underline{\nabla} \times \left[\sqrt{Ta}\left(\sin\theta\frac{\partial \mathbf{q}}{\partial z} + \cos\theta\frac{\partial \mathbf{q}}{\partial y}\right)\right] = \sqrt{Ta}\left(\sin\theta\frac{\partial \boldsymbol{\zeta}}{\partial z} + \cos\theta\frac{\partial \boldsymbol{\zeta}}{\partial y}\right). \tag{4.42}
$$

Substituting equations (4.39)-(4.42) into equation (4.38) we obtain,

$$
\begin{aligned}
\frac{1}{Pr}\left(\frac{\partial}{\partial t}(\nabla^2 \mathbf{q})\right) &= -\frac{\partial^2}{\partial x \partial z}(R_T T - R_S S)g_1(t)\mathbf{i} - \frac{\partial^2}{\partial y \partial z}(R_T T - R_S S)g_1(t)\mathbf{j} + \nabla^4 \mathbf{q} \\
&+ \nabla_H^2 (R_T T - R_S S)g_1(t)\mathbf{k} - \sqrt{Ta}\left(\sin\theta\frac{\partial \boldsymbol{\zeta}}{\partial z} + \cos\theta\frac{\partial \boldsymbol{\zeta}}{\partial y}\right),
\end{aligned}
\tag{4.43}
$$

where, $\boldsymbol{\zeta}$ is the vorticity vector and $\nabla_H^2 = \partial^2/\partial x^2 + \partial^2/\partial y^2$, where ∇_H^2 is called the horizontal Laplacian. The linearized $z-$ components of our system are as follows:

$$
\frac{1}{Pr}\left(\frac{\partial \zeta_z}{\partial t}\right) = \nabla^2 \zeta_z + \sqrt{Ta}\left(\sin\theta\frac{\partial w}{\partial z} + \cos\theta\frac{\partial w}{\partial y}\right), \tag{4.44}
$$

$$
\begin{aligned}
\frac{1}{Pr}\left(\frac{\partial}{\partial t}(\nabla^2 w)\right) =& \nabla_H^2 (R_T T - R_S S)g_1(t) + \nabla^4 w \\
&- \sqrt{Ta}\left(\sin\theta\frac{\partial \zeta_z}{\partial z} + \cos\theta\frac{\partial \zeta_z}{\partial y}\right),
\end{aligned}
\tag{4.45}
$$

$$
\frac{\partial T}{\partial t} - w = \nabla^2 T, \tag{4.46}
$$

$$
\frac{\partial S}{\partial t} - w = Le^{-1}\nabla^2 S. \tag{4.47}
$$

We assume a wave-like solution for the perturbations. That is,

$$\begin{aligned}
\zeta_z(t,x,y,z) &= Z(z)\exp\left[\sigma t + i(k_x x + k_y y)\right] \\
T(t,x,y,z) &= T(z)\exp\left[\sigma t + i(k_x x + k_y y)\right] \\
S(t,x,y,z) &= S(z)\exp\left[\sigma t + i(k_x x + k_y y)\right] \\
w(t,x,y,z) &= W(z)\exp\left[\sigma t + i(k_x x + k_y y)\right]
\end{aligned} \tag{4.48}$$

$$\nabla^2 = \frac{\partial^2}{\partial x^2} + \frac{\partial^2}{\partial y^2} + \frac{\partial^2}{\partial z^2} = \frac{d^2}{dz^2} - n^2, \tag{4.49}$$

where $W(z), T(z), S(z)$, and $Z(z)$ are the amplitudes, σ is the growth rate, $k_x,\ k_y$ are the horizontal wave-numbers and

$$n^2 = k_x^2 + k_y^2.$$

Perturbations of the initial state can grow or decay depending on σ. Substituting equations (4.48) into (4.44-4.47) we obtain the following set of equations,

$$\frac{1}{Pr}\sigma Z = (D^2 - n^2)Z + \sqrt{Ta}(\sin\theta D + ik_y\cos\theta)W, \tag{4.50}$$

$$\begin{aligned}
\frac{\sigma}{Pr}(D^2 - n^2)W = (D^2 - n^2)^2 W - n^2(R_T T - R_S S)g_1(t) \\
- \sqrt{Ta}(\sin\theta D + ik_y\cos\theta)Z,
\end{aligned} \tag{4.51}$$

$$\sigma T - W = (D^2 - n^2)T, \tag{4.52}$$

$$\sigma S - W = Le^{-1}(D^2 - n^2)S, \tag{4.53}$$

where

$$D(\cdot) = \frac{d}{dz}(\cdot).$$

Equations (4.50-4.53) consists of four equations for four unknowns $Z(z)$, $T(z)$, $S(z)$, and $W(z)$. We eliminate $Z(z)$ to obtain three equations for three unknowns. Equation (4.50) can be rewritten as follows,

$$\left(D^2 - n^2 - \frac{\sigma}{Pr}\right) Z = -\sqrt{Ta}(\sin\theta D + ik_y\cos\theta)W. \tag{4.54}$$

Operating on equation (4.51) by

$$\left(D^2 - n^2 - \frac{\sigma}{Pr}\right),$$

yields the following equation,

$$\begin{aligned}
\frac{1}{Pr}(D^2 - n^2)\left(D^2 - n^2 - \frac{\sigma}{Pr}\right) W = (D^2 - n^2)^2 \left(D^2 - n^2 - \frac{\sigma}{Pr}\right) W \\
- n^2 \left(D^2 - n^2 - \frac{\sigma}{Pr}\right)(R_T T - R_S S)g_1(t) \\
+ Ta(\sin\theta D + ik_y\cos\theta)^2 W,
\end{aligned} \tag{4.55}$$

which does not depend on $Z(z)$. Equations (4.52, 4.53, and 4.55) form three equations for three unknowns $T(z)$, $S(z)$, and $W(z)$.

4.5 Boundary conditions

Chandrasekhar [6] discussed all possible boundary conditions for a convection process. He noted that sometimes it may be necessary to employ unrealistic boundary conditions to obtain an analytical solution. There are two types of boundaries: rigid surfaces, where no-slip occurs, and free boundaries, where no tangential stress occurs. We first examine all the possible boundary conditions satisfied by both rigid and free surfaces, and then later we will consider the ones suitable for our problem.

4.5.1 Boundary conditions satisfied at both rigid and free surfaces

Consider physical variables at $z = 0$:

$$\begin{aligned} w(t,x,y,0) &= 0 && \text{no cavities form,} \\ T'(t,x,y,0) &= 0 && \text{surface maintained at constant temperature,} \\ S'(t,x,y,0) &= 0 && \text{surface maintained at constant salinity,} \end{aligned} \tag{4.56}$$

and at $z = d$:

$$\begin{aligned} w(t,x,y,d) &= 0 && \text{so cavities form,} \\ T'(t,x,y,d) &= 0 && \text{surface maintained at constant temperature,} \\ S'(t,x,y,d) &= 0 && \text{surface maintained at constant salinity.} \end{aligned} \tag{4.57}$$

The surfaces $z = 0$ and $z = d$ are maintained at constant temperatures and salinities and therefore do not undergo a perturbation. The normal component of velocity must vanish on these surfaces.

4.5.2 Boundary conditions satisfied at rigid surfaces

Suppose that $z = 0$ is a rigid surface, then no-slip occurs:

$$\begin{aligned} u(t,x,y,0) &= 0, \\ v(t,x,y,0) &= 0. \end{aligned} \tag{4.58}$$

But (4.58) holds for all values of x and y. Thus we can differentiate (4.58) with respect to x and y. Hence

$$\begin{aligned} \frac{\partial u}{\partial x}(t,x,y,0) &= 0. \\ \frac{\partial v}{\partial y}(t,x,y,0) &= 0. \end{aligned} \tag{4.59}$$

But the continuity equation at $z = 0$ is,

$$\frac{\partial u}{\partial x}(t,x,y,0) + \frac{\partial v}{\partial y}(t,x,y,0) + \frac{\partial w}{\partial z}(t,x,y,0) = 0. \tag{4.60}$$

Hence,

$$\frac{\partial w}{\partial z}(t,x,y,0) = 0. \tag{4.61}$$

Thus, if $z = 0$ and $z = d$ are rigid surfaces,

$$\frac{\partial w}{\partial z}(t, x, y, 0) = 0, \quad \text{and} \quad \frac{\partial w}{\partial z}(t, x, y, d) = 0. \tag{4.62}$$

Now consider the boundary conditions on the $z-$component of vorticity $\boldsymbol{\zeta}$,

$$\begin{aligned} \boldsymbol{\zeta} &= \underline{\nabla} \times \mathbf{q} \\ &= \mathbf{i}\left[\frac{\partial w}{\partial y} - \frac{\partial v}{\partial z}\right] + \mathbf{j}\left[\frac{\partial u}{\partial z} - \frac{\partial w}{\partial x}\right] + \mathbf{k}\left[\frac{\partial v}{\partial x} - \frac{\partial u}{\partial y}\right]. \end{aligned} \tag{4.63}$$

Thus

$$\zeta_x = \frac{\partial w}{\partial y} - \frac{\partial v}{\partial z}, \qquad \zeta_y = \frac{\partial u}{\partial z} - \frac{\partial w}{\partial x}, \qquad \zeta_z = \frac{\partial v}{\partial x} - \frac{\partial u}{\partial y}. \tag{4.64}$$

Suppose $z = 0$ is a rigid surface, then since (4.58) is satisfied for all x and y,

$$\frac{\partial u}{\partial y}(t, x, y, 0) = 0, \qquad \frac{\partial v}{\partial x}(t, x, y, 0) = 0, \tag{4.65}$$

and therefore

$$\begin{aligned} \zeta_z(t, x, y, 0) &= \frac{\partial v}{\partial x}(t, x, y, 0) - \frac{\partial u}{\partial y}(t, x, y, 0) \\ &= 0. \end{aligned} \tag{4.66}$$

Hence if $z = 0$ and $z = d$ are rigid,

$$\zeta_z(t, x, y, 0) = 0, \quad \text{and} \quad \zeta_z(t, x, y, d) = 0. \tag{4.67}$$

4.5.3 Boundary conditions satisfied at free surfaces

On a free surface there are no tangential stresses. Suppose that $z = 0$ is a free surface, then

$$\tau_{zx}(t, x, y, 0) = 0, \quad \text{and} \quad \tau_{zy}(t, x, y, 0) = 0. \tag{4.68}$$

From the Navier-Poisson law for an incompressible fluid,

$$\begin{aligned} \tau_{ik} &= -p\delta_{ik} + 2\mu D_{ik} \\ &= -p\delta_{ik} + \mu\left(\frac{\partial q_i}{\partial x_k} + \frac{\partial q_k}{\partial x_i}\right), \end{aligned} \tag{4.69}$$

where,

$$D_{ik} = \frac{1}{2}\left(\frac{\partial q_i}{\partial x_k} + \frac{\partial q_k}{\partial x_i}\right), \tag{4.70}$$

thus,

$$\tau_{zx} = \mu\left(\frac{\partial w}{\partial x} + \frac{\partial u}{\partial z}\right), \qquad \tau_{zy} = \mu\left(\frac{\partial w}{\partial y} + \frac{\partial v}{\partial z}\right). \tag{4.71}$$

At $z = 0$ we have from (4.71),

$$\frac{\partial w}{\partial x}(t,x,y,0) + \frac{\partial u}{\partial z}(t,x,y,0) = 0, \quad \text{and} \quad \frac{\partial w}{\partial y}(t,x,y,0) + \frac{\partial v}{\partial z}(t,x,y,0) = 0. \tag{4.72}$$

But since no cavities form at $z = 0$,

$$w(t,x,y,0) = 0, \tag{4.73}$$

for all x and y. Therefore differentiating with respect to x and y yields the following,

$$\frac{\partial w}{\partial x}(t,x,y,0) = 0, \quad \text{and} \quad \frac{\partial w}{\partial y}(t,x,y,0) = 0. \tag{4.74}$$

Hence, from (4.72),

$$\frac{\partial u}{\partial z}(t,x,y,0) = 0, \quad \text{and} \quad \frac{\partial v}{\partial z}(t,x,y,0) = 0. \tag{4.75}$$

Now the continuity equation is,

$$\frac{\partial u}{\partial x}(t,x,y,z) + \frac{\partial v}{\partial y}(t,x,y,z) + \frac{\partial w}{\partial z}(t,x,y,z) = 0. \tag{4.76}$$

Now differentiating it with respect to z we obtain,

$$\frac{\partial}{\partial x}\left(\frac{\partial u}{\partial z}(t,x,y,z)\right) + \frac{\partial}{\partial y}\left(\frac{\partial v}{\partial z}(t,x,y,z)\right) + \frac{\partial^2 w}{\partial z^2}(t,x,y,z) = 0. \tag{4.77}$$

Set $z = 0$. Then

$$\frac{\partial}{\partial x}\left(\frac{\partial u}{\partial z}(t,x,y,0)\right) + \frac{\partial}{\partial y}\left(\frac{\partial v}{\partial z}(t,x,y,0)\right) + \frac{\partial^2 w}{\partial z^2}(t,x,y,0) = 0. \tag{4.78}$$

by applying (4.75) the following boundary condition is obtained,

$$\frac{\partial^2 w}{\partial z^2}(t,x,y,0) = 0. \tag{4.79}$$

Next we derive a boundary condition on ζ_z at a free surface. From (4.64),

$$\zeta_z = \frac{\partial v}{\partial x} - \frac{\partial u}{\partial y}, \tag{4.80}$$

and differentiate with respect to z we obtain,

$$\frac{\partial \zeta_z}{\partial z}(t,x,y,z) = \frac{\partial}{\partial x}\left(\frac{\partial v}{\partial z}(t,x,y,z)\right) - \frac{\partial}{\partial y}\left(\frac{\partial u}{\partial z}(t,x,y,z)\right). \tag{4.81}$$

Set $z = 0$, then after differentiation gives

$$\begin{aligned}\frac{\partial \zeta_z}{\partial z}(t,x,y,0) &= \frac{\partial}{\partial x}\left(\frac{\partial v}{\partial z}(t,x,y,0)\right) - \frac{\partial}{\partial y}\left(\frac{\partial u}{\partial z}(t,x,y,0)\right) \\ &= 0.\end{aligned} \tag{4.82}$$

and applying equation (4.74) we obtain the boundary condition

$$\frac{\partial \zeta_z(t,x,y,0)}{\partial z} = 0. \tag{4.83}$$

4.5.4 Summary of boundary conditions

- Both rigid and free surfaces.

$$w = 0, \quad T' = 0, \quad \text{and} \quad S' = 0. \tag{4.84}$$

- Rigid surfaces.

$$u = 0, \quad v = 0, \quad \frac{\partial w}{\partial z} = 0, \quad \text{and} \quad \zeta_z = 0. \tag{4.85}$$

- Free surfaces.

$$\frac{\partial u}{\partial z} = 0 \quad \frac{\partial v}{\partial z} = 0 \quad \frac{\partial^2 w}{\partial z^2} = 0 \quad \text{and} \quad \frac{\partial \zeta_z}{\partial z} = 0. \tag{4.86}$$

4.6 Application of the boundary conditions

The solution to equations (4.52, 4.53, and 4.55) is assumed to be periodic and sine-like. We assume stress-free boundary conditions on the upper boundary $z = 1$ and on the lower boundary $z = 0$. We also assume that the perturbations $W(z)$, $T(z)$, and $S(z)$ vanish on the upper and lower boundaries. Hence,

$$\begin{aligned} z = 1: \quad & W(1) = 0, \quad \frac{d^2W}{dz^2}(0) = 0, \quad T(1) = 0, \quad S(1) = 0 \\ z = 0: \quad & W(0) = 0, \quad \frac{d^2W}{dz^2}(0) = 0, \quad T(0) = 0, \quad S(0) = 0. \end{aligned} \tag{4.87}$$

Thus, we look for solutions of the form,

$$\begin{aligned} W(z) &= W_0 \sin \pi z, \\ T(z) &= T_0 \sin \pi z, \\ S(z) &= S_0 \sin \pi z. \end{aligned} \tag{4.88}$$

Subject to the stress-free boundary conditions(4.87). Where W_0, T_0, and S_0 are constants. This form of solution satisfies the boundary conditions in (4.87). Substituting equations (4.88) into (4.52, 4.53, and 4.55) we obtain the following

$$\begin{aligned} \frac{\sigma}{Pr}\left[\pi^2 + n^2 + \sigma Pr^{-1}\right](\pi^2 + n^2)W_0 \sin \pi z &= \left[(\pi^2 + n^2 + \sigma Pr^{-1}\right](\pi^2 + n^2)W_0 \sin \pi z \\ &+ n^2\left(\pi^2 + n^2 + \sigma Pr^{-1}\right)(R_T T - R_S S) g_1(t) \sin \pi z \\ &- Ta\left[k_y \cos^2\theta - \pi^2 \sin^2\theta\right] W_0 \sin \pi z + i\, Ta\, W_0\, k_y \sin 2\theta \cos \pi z. \end{aligned} \tag{4.89}$$

Equation (4.89) is of the form,

$$A \sin \pi z + B \cos \pi z = 0, \tag{4.90}$$

where A and B are constants independent of z and,

$$\begin{aligned} A = & \left[(\pi^2 + n^2 + \sigma Pr^{-1})^2(\pi^2 + n^2) + Ta(k_y \cos^2\theta + \pi^2 \sin^2\theta)\right] W_0 \\ & + n^2(\pi^2 + n^2 + \sigma Pr^{-1}) g_1(t)(R_S S_0 - R_T T_0), \end{aligned} \tag{4.91}$$

and

$$B = 2ik_y Ta W_0(\sin\theta\cos\theta). \tag{4.92}$$

To obtain a solution for A and B, we set $z = 0$ which gives

$$B = 0,$$

and therefore

$$A = 0.$$

Thus

$$2ik_y Ta W_0(\sin\theta\cos\theta) = 0, \tag{4.93}$$

and

$$\begin{aligned} & \left[(\pi^2 + n^2 + \sigma Pr^{-1})^2(\pi^2 + n^2) + Ta(k_y \cos^2\theta + \pi^2 \sin^2\theta)\right] W_0 \\ & + n^2(\pi^2 + n^2 + \sigma Pr^{-1}) g_1(t)(R_S S_0 - R_T T_0) = 0, \end{aligned} \tag{4.94}$$

$$W_0 - (\pi^2 + n^2 + \sigma)T_0 = 0, \tag{4.95}$$

$$W_0 - (Le^{-1}(\pi^2 + n^2) + \sigma)S_0 = 0. \tag{4.96}$$

Equations (4.94, 4.95 and 4.96) form a system of three linear equations for W_0, T_0, and S_0. Let

$$k_y \cos^2\theta + \pi^2 \sin^2\theta = \Theta, \tag{4.97}$$

and

$$\pi^2 + n^2 = \Psi$$

then the system is given by

$$\mathbf{Az} = \mathbf{0}, \tag{4.98}$$

where $\mathbf{A}$ is given by,

$$\begin{bmatrix} \left[(\Psi + \sigma Pr^{-1})^2\Psi + Ta\Theta\right] & -n^2(\Psi + \sigma Pr^{-1})g_1(t)R_T & n^2(\Psi + \sigma Pr^{-1})g_1(t)R_S \\ 1 & -(\Psi + \sigma) & 0 \\ 1 & 0 & -(Le^{-1}\Psi + \sigma) \end{bmatrix}, \tag{4.99}$$

where

$$\mathbf{z} = \begin{bmatrix} W_0 \\ T_0 \\ S_0 \end{bmatrix}, \quad \text{and} \quad \mathbf{0} = \begin{bmatrix} 0 \\ 0 \\ 0 \end{bmatrix}.$$

A non-trivial solution exists provided

$$det(\mathbf{A}) = 0.$$

Therefore,

$$\begin{aligned}&n^2(\Psi+\sigma Pr^{-1})g_1(t)R_S(\Psi+\sigma)-n^2(\Psi+\sigma Pr^{-1})g_1(t)R_T(Le^{-1}\Psi+\sigma)\\&\left[(\Psi+\sigma Pr^{-1})^2\Psi+Ta\Theta\right](Le^{-1}\Psi+\sigma)(\Psi+\sigma)=0.\end{aligned} \tag{4.100}$$

Equation (4.100) can be solved for R_T in terms of R_S.

$$R_T=\frac{\left[(\Psi+\sigma Pr^{-1})^2\Psi+Ta\Theta\right](\Psi+\sigma)}{n^2(\Psi+\sigma Pr^{-1})g_1(t)}+R_S\frac{\Psi+\sigma}{Le^{-1}\Psi+\sigma}. \tag{4.101}$$

Equation (4.100) can be written as a fourth-order polynomial with real coefficients.

$$p_4(\sigma)=0, \tag{4.102}$$

where,

$$p_4(\sigma)=\sigma^4+B_1\sigma^3+B_2\sigma^2+B_3\sigma+B_4, \tag{4.103}$$

and

$$B_1=(\pi^2+n^2)[1+2Pr+Le^{-1}], \tag{4.104}$$

$$\begin{aligned}B_2=&(\pi^2+n^2)^2[Le^{-1}+2Pr(1+Le^{-1})+Pr^2]+\frac{Pr^2}{(\pi^2+n^2)}Ta\left(k_y\cos^2\theta+\pi^2\sin^2\theta\right)\\&-\frac{Pr\,n^2}{(\pi^2+n^2)}g_1(t)[R_T-R_S],\end{aligned} \tag{4.105}$$

$$\begin{aligned}B_3=&Pr^2(\pi^2+n^2)^3\left[\frac{2}{PrLe}+\frac{1}{Le}+1\right]+Pr(1+Le^{-1})Ta[k_y\cos^2\theta+\pi^2\sin^2\theta]\\&-n^2Pr^2g_1(t)\left[\left(\frac{1}{PrLe}+1\right)R_T-\left(\frac{1}{Pr}+1\right)R_S\right],\end{aligned} \tag{4.106}$$

and

$$B_4=Pr^2(\pi^2+n^2)Le^{-1}\left[(\pi^2+n^2)^3+Ta(k_y\cos^2\theta+\pi^2\sin^2\theta)-n^2(R_T-LeR_S)g_1(t)\right]. \tag{4.107}$$

When $Ta=0$ the polynomial is of order three [16]. It is of order four when $Ta\neq 0$. Equation (4.103) has four roots.

It has either four real roots,

$$\sigma_1,\quad \sigma_2,\quad \sigma_3,\quad \text{and}\quad \sigma_4, \tag{4.108}$$

or two real roots and two complex conjugate roots,

$$\sigma_1,\quad \sigma_2,\quad \sigma_3+i\sigma_4\quad \text{and}\quad \sigma_3-i\sigma_4, \tag{4.109}$$

or two sets of complex conjugate roots,

$$\sigma_1+i\sigma_2,\quad \sigma_1-i\sigma_2,\quad \sigma_3+i\sigma_4,\quad \text{and}\quad \sigma_3-i\sigma_4. \tag{4.110}$$

When,

$$\sigma = \sigma_R + i\sigma_I, \tag{4.111}$$

then the solution is of the form,

$$\begin{bmatrix} W(t,x,y,z) \\ T(t,x,y,z) \\ S(t,x,y,z) \end{bmatrix} = \begin{bmatrix} W_0 \\ T_0 \\ S_0 \end{bmatrix} \left(\exp\left[\sigma_R t + i(\sigma_I t + k_y y + k_x x)\right]\right). \tag{4.112}$$

If $\sigma_R < 0$, the perturbation will decrease in magnitude and the system will eventually return to its initial state. The initial state is *stable* with respect to this perturbation. If $\sigma_R > 0$, the perturbation will increase in amplitude and progressively depart from the initial state. The initial state is *unstable* and we will have resonance when the amplitude grows unbounded. A system is considered stable if it is stable with respect to every possible perturbation to which it can be subjected. A system is unstable if there is at least one unstable perturbation state to which it can be subjected [6].

The condition

$$\sigma_R = 0, \tag{4.113}$$

separates the two states and defines a state of marginal stability or neutral stability. The states of marginal stability can be of two kinds, stationary and oscillatory.

Stationary phase: $\sigma_I = 0$. The amplitude of small disturbances grows steadily over time. The transition from stability to instability is by a marginal state with a stationary pattern of motions. The principle of the exchange of instability is valid. Instability sets in as a stationary cellular convection or secondary flow.

Oscillatory phase: $\sigma_I \neq 0$. The amplitude of small disturbances grows by oscillations of increasing (decreasing) amplitude. The transition from stability to instability is by a marginal state exhibiting oscillatory motions with a certain definite frequency. If unstable oscillatory motion occurs at the onset, one has a case of *overstability*. A slight displacement provokes restoring forces tending away from equilibrium. In overstability, the forces are so strong as to overshoot the corresponding position in the other equilibrium site.

4.7 Summary

In this chapter, we have imposed normal modes analysis studied in Chapter 2 on the governing equations derived in Chapter 3. We further discussed three types of boundary conditions, rigid-rigid, rigid-free, and free-free (no-slip) boundary conditions. In this work, we have decided to impose the no-slip boundary conditions. By doing so, we have derived the thermal Rayleigh number, a paramount parameter in convective stability analysis. The Rayleigh number here is found to be dependent on the Prandtl number, the Lewis number, the salinity Rayleigh number, and the rotation parameter (Ta) together with time-dependent sinusoidal periodic gravitational acceleration. We introduced the growth parameter (σ).

Chapter 5

Stationary convection

5.1 Introduction

In this chapter, we will conduct a stability analysis on stationary convection introduced in Chapter 4. Our point of departure is the stability parameter, the Rayleigh number in equation (4.101). We will compare this Rayleigh number with the critical Rayleigh number ($R_c = 27\pi^4/4$). If $R_T^{sc} > R_c$ this implies that the system is unstable and if $R_T^{sc} < R_c$ then the system is stable. we will vary the different parameters to deduce the effect of each on stability analysis.

5.2 Analysis

We deduce the onset of stationary convection by setting $\sigma = 0$ in equation (4.101). Then we obtain,

$$R_T^{sc} = \frac{\Psi^3 + Ta\Theta}{n^2 g_1(t)} + R_S Le, \tag{5.1}$$

where $\Psi = \pi^2 + n^2$, and R_T^{sc} is the Rayleigh number for the exchange of instability. We obtain the critical wave number (n) by minimizing R_T^{sc} with respect to n^2, that is

$$\frac{\partial R_T^{sc}}{\partial n^2} = \frac{3(\pi^2 + n^2)^2 n^2 - [(\pi^2 + n^2)^3 + Ta\Theta]}{n^4 g_1(t)} = 0, \tag{5.2}$$

therefore,

$$3(\pi^2 + n^2)^2 n^2 - [(\pi^2 + n^2)^3 + Ta\Theta] = 0. \tag{5.3}$$

From Equation (5.3), we can deduce that the critical wave number is independent of gravity modulation but depends on the Taylor number, denoted as Ta. Thus, rotation plays a significant role in determining the critical wave number. In the absence of rotation ($Ta = 0$), the critical wave number is given by,

$$n = \frac{\pi}{\sqrt{2}}. \tag{5.4}$$

The corresponding Rayleigh number in the absence of gravity modulation, rotation, and salinity is given by

$$R_c = \frac{27}{4}\pi^4 \approx 657.51, \tag{5.5}$$

which is consistent with the literature [53]. For different values of $Ta\Theta$, one can solve equation (5.3). Consider equation (4.93). The equation is satisfied if one of the following is true,

$$\begin{aligned} k_y &= 0 \\ \theta &= 0 \\ \theta &= \pm\pi/2, \end{aligned} \tag{5.6}$$

where $\theta = 0$ means we are at the equator, $\theta = \pm\pi/2$ means we are at the poles, and $k_y = 0$ means no waves in the $y-$direction.

5.3 Stationary convection analysis at the equator

Consider the case where $\theta = 0$. This case corresponds to the equatorial region of the Earth. Thus $\Theta = k_y$ and equation (5.1) becomes,

$$R_T^{sc} = \frac{(\pi^2 + n^2)^3 + Tak_y}{n^2 g_1(t)} + R_S Le. \tag{5.7}$$

To find the minimum of R_T^{sc}, we find the non-trivial point (k_x, k_y) that minimizes R_T^{sc}. That is, we compute

$$\frac{\partial R_T^{sc}}{\partial k_x} = 0 \quad \text{and} \quad \frac{\partial R_T^{sc}}{\partial k_y} = 0.$$

Now,

$$\begin{aligned} \frac{\partial R_T^{sc}}{\partial k_x} &= \frac{6k_x}{n^4 g_1(t)}(\pi^2 + k_y^2 + k_x^2)^2(k_y^2 + k_x^2) - \frac{2k_x}{n^4 g_1(t)}(\pi^2 + k_y^2 + k_x^2)^3 - \frac{2Tak_y k_x}{n^4 g_1(t)} \\ &= 0, \end{aligned} \tag{5.8}$$

and

$$\begin{aligned} \frac{\partial R_T^{sc}}{\partial k_y} &= \frac{(Ta + 6k_y(\pi^2 + k_y^2 + k_x^2)^2)(k_y^2 + k_x^2)}{n^4 g_1(t)} - \frac{2k_y(\pi^2 + k_y^2 + k_x^2)^3 - 2Tak_y^2}{n^4 g_1(t)} \\ &= 0. \end{aligned} \tag{5.9}$$

Equation (5.8) is satisfied if,

$$k_x = 0, \quad \text{and} \quad 6(\pi^2 + k_y^2 + k_x^2)^2(k_y^2 + k_x^2) - 2(\pi^2 + k_y^2 + k_x^2)^3 - 2Tak_y \neq 0, \tag{5.10}$$

$$k_x \neq 0, \quad \text{and} \quad 6(\pi^2 + k_y^2 + k_x^2)^2(k_y^2 + k_x^2) - 2(\pi^2 + k_y^2 + k_x^2)^3 - 2Tak_y = 0, \tag{5.11}$$

or,

$$k_x = 0, \quad \text{and} \quad 6(\pi^2 + k_y^2 + k_x^2)^2(k_y^2 + k_x^2) - 2(\pi^2 + k_y^2 + k_x^2)^3 - 2Tak_y = 0. \tag{5.12}$$

Consider the first case (5.10). Substitute $k_x = 0$ into equation (5.9) to obtain the following expression,

$$\left[Ta + 6k_y(\pi^2 + k_y^2)^2\right](k_y^2) - 2k_y(\pi^2 + k_y^2)^3 - 2Tak_y^2 = 0, \tag{5.13}$$

which is satisfied for

$$k_y = 0,$$

or

$$\left[Ta + 6k_y(\pi^2 + k_y^2)^2\right](k_y) - 2(\pi^2 + k_y^2)^3 - 2Tak_y = 0.$$

For $k_y = 0$ we have the stationary point at

$$(k_x, k_y) = (0, 0)$$

which leads to a trivial solution. To obtain nontrivial solutions, we consider

$$\left[Ta + 6k_y(\pi^2 + k_y^2)^2\right](k_y) - 2(\pi^2 + k_y^2)^3 - 2Tak_y = 0, \tag{5.14}$$

which reduces to,

$$4k_y^6 + 6\pi^2 k_y^4 - 2\pi^6 - k_y Ta = 0. \tag{5.15}$$

The solution to equation (5.15) for various values of Ta is given in table (5.1). The plot indicates a strong linear relationship between k_y and Ta (see Figure 5.1), as evidenced by the equation

$$k_y = 0.000558292472727279 1 \times Ta + 2.221621177272728$$

and a remarkably high correlation coefficient of

$$r = 0.9999821717072658.$$

Ta	k_y
0	2.22144147
10	2.22713261
20	2.23279944
30	2.23844208
40	2.24406062
50	2.24965517
60	2.25522585
70	2.26077277
80	2.26629602
90	2.27179574
100	2.27727204

Table 5.1: *Values of k_y for different values of Ta*

The horizontal wavelengths in the ocean can range from 1×10^{-4} to 5×10^{-2}, while the Taylor number can range anywhere between $(1 \text{ and } 10^4)$[53]. In the following plots,

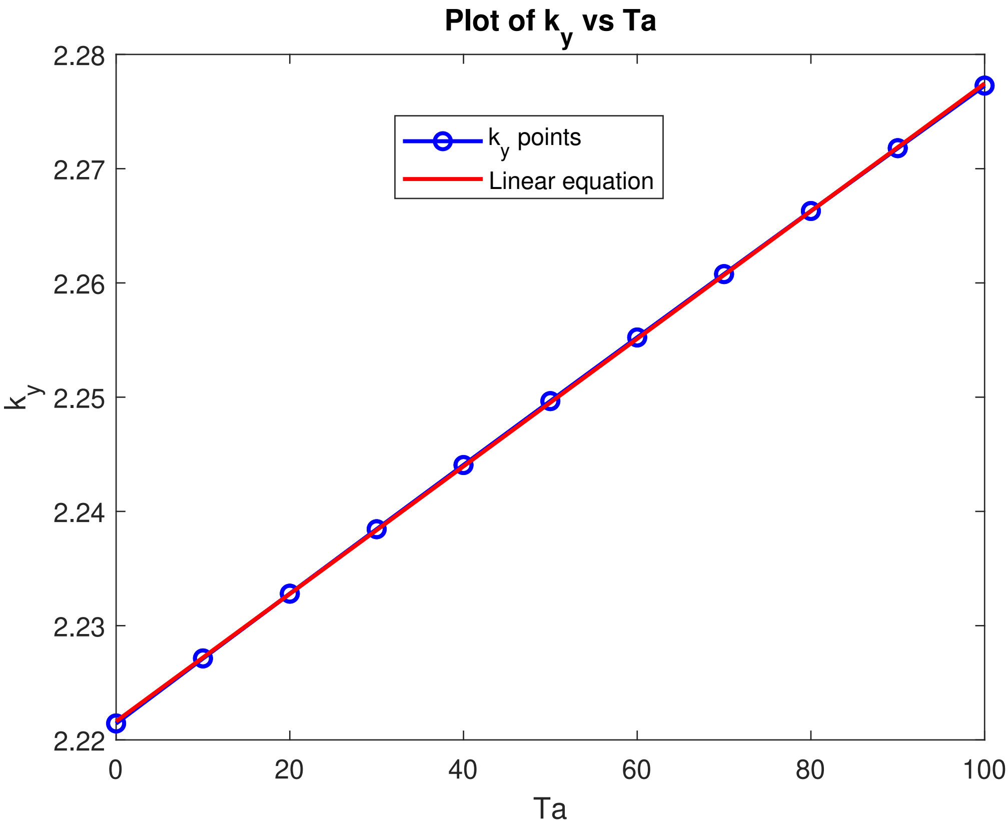

Figure 5.1: *Critical wave number* k_y *plotted against the Taylor number* Ta

we assume constant gravity with $R_S = 100$, $n = (0.5, 8)$.

The second and third cases (5.11 and 5.12) lead to a trivial solution

$$(k_x^2 + k_y^2)Ta = 0. \tag{5.16}$$

Thus,

$$(k_x, k_y) = (0, 0). \tag{5.17}$$

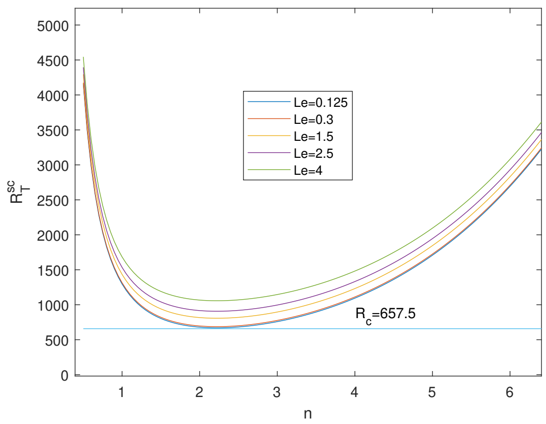

(a) No rotation

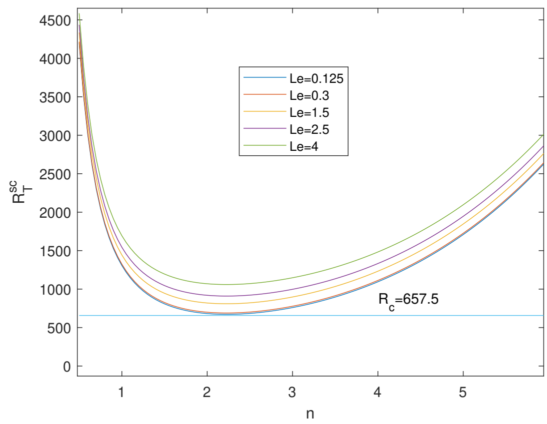

(b) $Ta = 10$

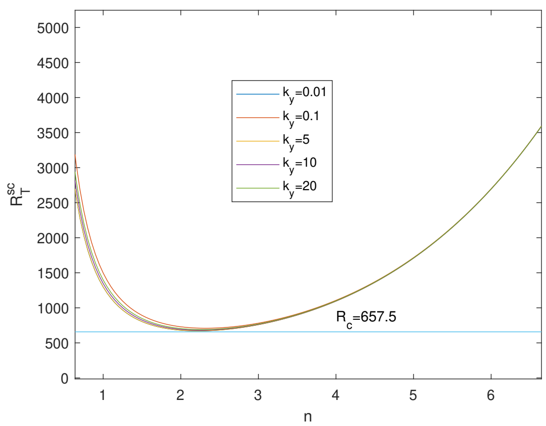

(c) $Ta = 20$

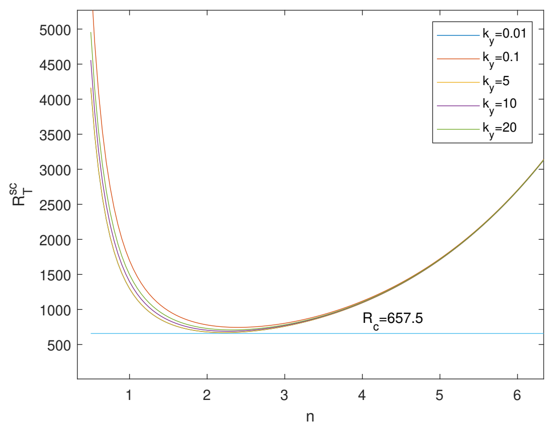

(d) $Ta = 30$

Figure 5.2: *The Rayleigh number plotted against the wave number (n) with and without rotation for stationary convection.*

From Figure (5.2), it is evident that a direct relationship exists between the Rayleigh number and the Lewis number. The influence of the Lewis number affects the system's behavior, potentially signifying a shift in stability. Furthermore, it can be inferred that the impact of the Lewis number remains unaffected by rotation. The horizontal wave number (k_y) exerts an additional influence, distinct from the wave number (n), on the system's stability at the equator. This influence is dependent upon the system's rotation.

The effects of gravity modulation on the stability of a stationary convection process can be seen through a variation in the amplitude (δ) and frequency (ω_m). We will restrict the product ($\omega_m t$) between $(0, 2\pi)$ [54].

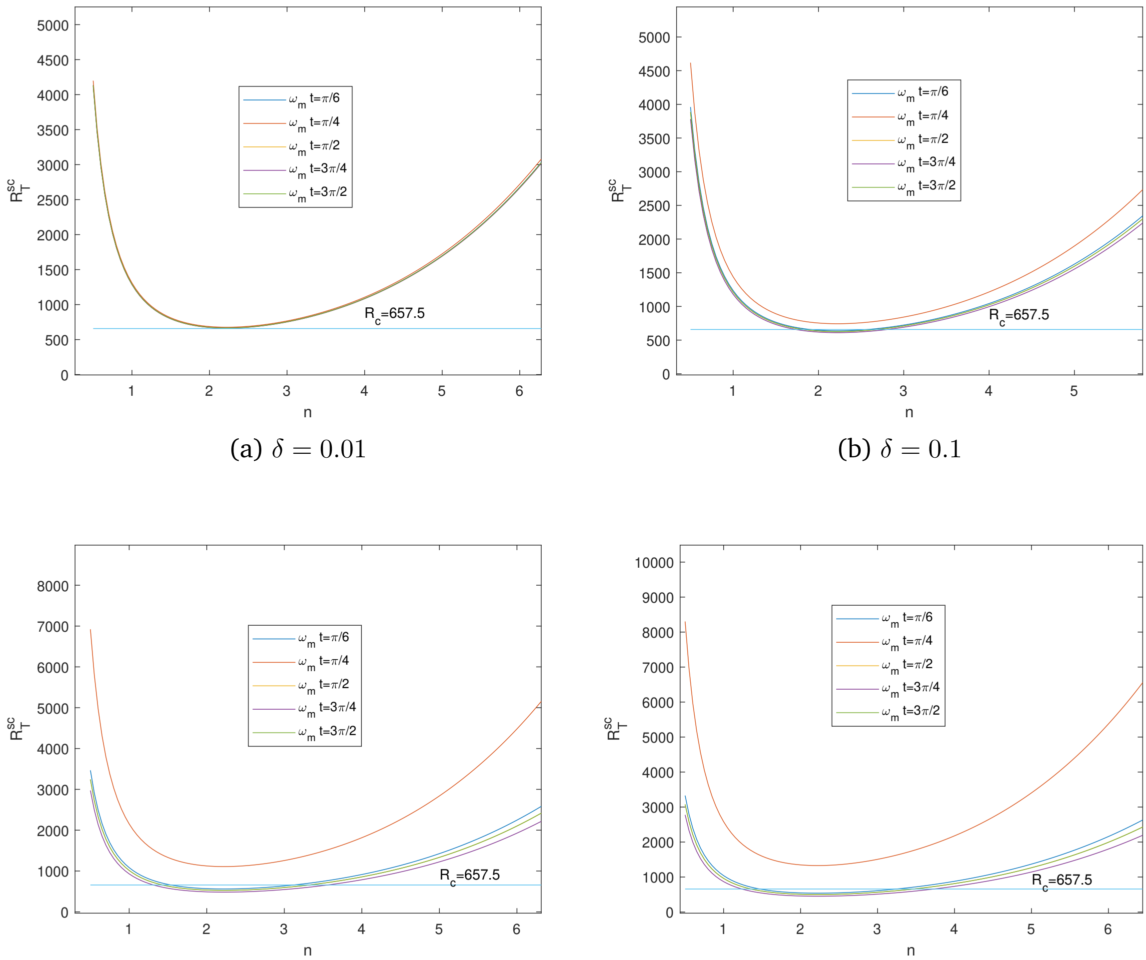

(a) $\delta = 0.01$

(b) $\delta = 0.1$

(c) $\delta = 0.4$

(d) $\delta = 0.5$

Figure 5.3: *The Rayleigh number plotted against the wave number (n) at different modulation amplitude for stationary convection.*

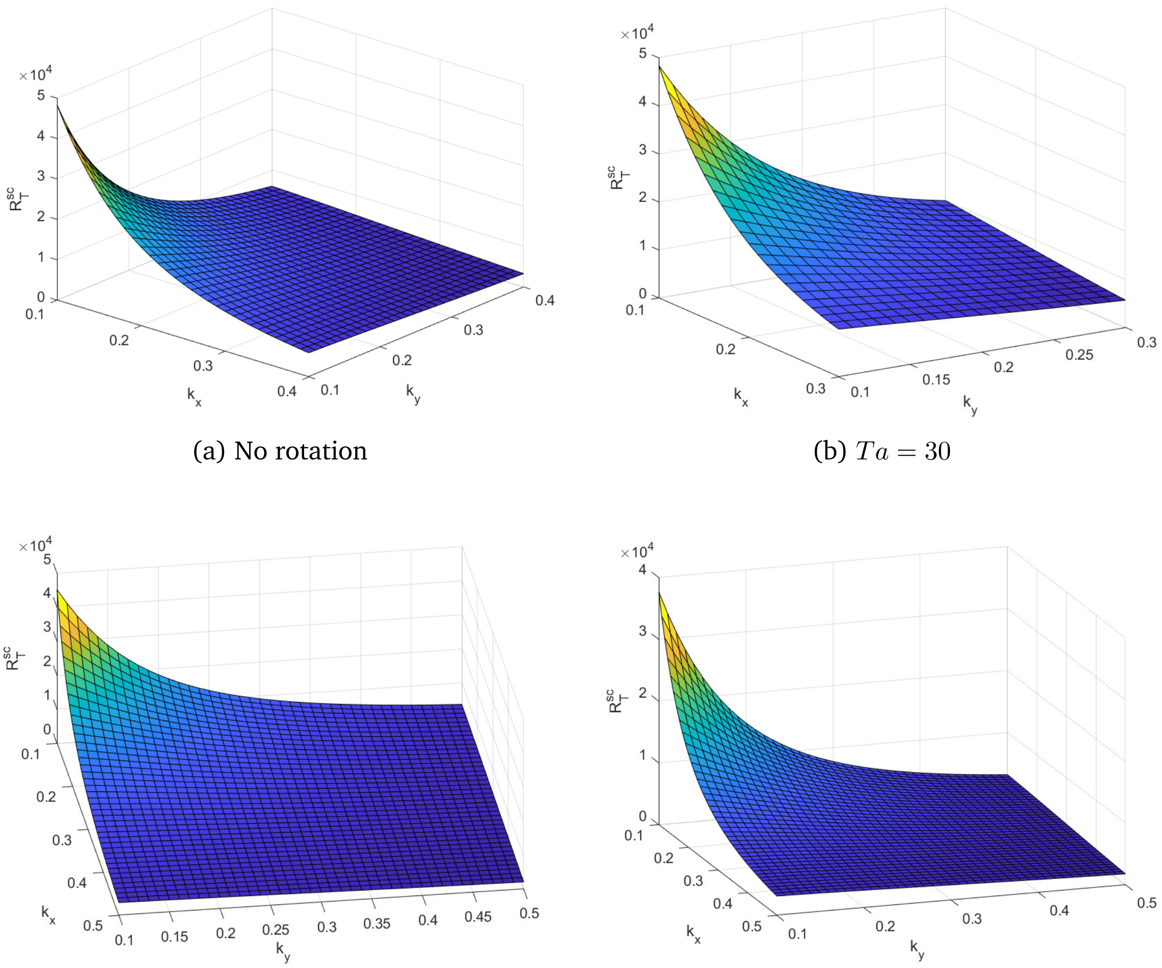

(a) No rotation

(b) $Ta = 30$

(c) $\delta = 0.1, \quad$ and $\quad \omega_m t = \frac{\pi}{4}$.

(d) $\delta = 0.01, \quad$ and $\quad \omega_m t = \frac{\pi}{4}$.

Figure 5.4: *The Rayleigh number plotted against the horizontal wave numbers(k_x and k_y) for stationary convection.*

Figure 5.4 illustrates the variation of the Rayleigh number for stationary convection with k_x and k_y. With smaller wave numbers, we observe higher Rayleigh numbers. In the context of gravity modulation, significant Rayleigh numbers result from minor variations. For instance, at $\delta = 0.1$ and $\omega_m t = \pi/4$, we achieve $1 + \delta \sin \omega_m t = 1.0707$, and for $\delta = 0.4$ and $\omega_m t = \pi/4$, we reach $1 + \delta \sin \omega_m t = 1.2828$. Despite their small magnitudes, these variations substantially impact the stability of the process.

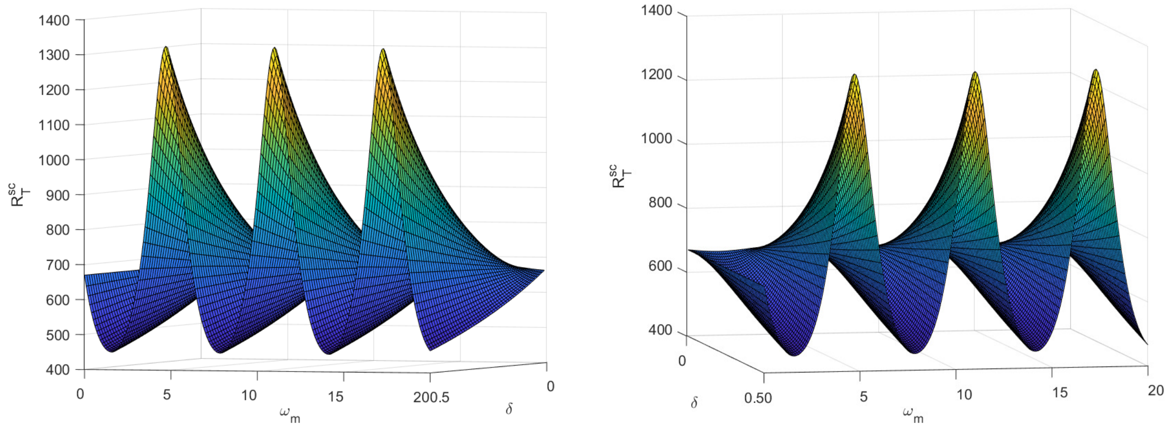

(a) No rotation (b) With rotation

Figure 5.5: *The Rayleigh number for stationary convection against the frequency and amplitude of modulation.*

The function $R_T(\delta, \omega_m)$ demonstrates independence from rotation. Figure 5.5 above shows a recurring, periodic pattern. This periodicity arises from the inherent cyclic behavior of the sine function. The outcomes suggest that, over time, the modulation of gravity will cyclically repeat, manifesting at intervals corresponding to multiples of 2π. However, this deduction appears impractical as it results in a sequence of repetitions yielding identical values. Consequently, the chosen gravity modulation form may be inappropriate. Despite the inadequacy of the chosen form, an essential insight offered by the equation is the establishment of both a lower and an upper bound, establishing a reasonable range for slight variations.

5.4 Stationary convection analysis at the poles

Consider the scenario where $\theta = \pm\pi/2$. This situation specifically pertains to the polar regions of the Earth. When $\theta = \pm\pi/2$, equation (5.1) transforms into,

$$R_T^{sc} = \frac{(\pi^2 + n^2)^3 + Ta\pi^2}{n^2(1 + \delta \sin \omega_m t)} + R_S Le. \tag{5.18}$$

We find the value of n where the function is minimum. Since R_T^{sc} is a function of n^2 we minimize it with respect to n^2. To do this, we take the derivative of R_T^{sc} with respect to n^2 and set it to zero:

$$\begin{aligned} \frac{dR_T^{sc}}{dn^2} &= \frac{1}{g_1(t)} \frac{3n^2(\pi^2 + n^2)^2 - (\pi^2 + n^2)^3 - Ta\pi^2}{n^4} \\ &= 0. \end{aligned} \tag{5.19}$$

We expand to obtain,

$$\frac{1}{n^4 g_1(t)} \left[2n^6 + 3\pi^2 n^4 - \pi^2(\pi^4 + Ta)\right] = 0. \tag{5.20}$$

Therefore,
$$2n^6 + 3\pi^2 n^4 - \pi^2(\pi^4 + Ta) = 0. \tag{5.21}$$
Let,
$$P_6(n) = 2n^6 + 3\pi^2 n^4 - \pi^2(\pi^4 + Ta). \tag{5.22}$$
Using Descartes' Rule of Signs which states that the potential count of positive roots in a polynomial is either equal to the number of sign alterations in its coefficients or less than that count by a multiple of 2. We deduce the possible number of positive roots for $P_6(n)$. Thus the number of possible roots for $P_6(n)$ is less than or equal to one. But since,
$$P_6(0) = -\pi^2(\pi^4 + Ta), \tag{5.23}$$
and
$$P_6(n \to \infty) = \infty, \tag{5.24}$$
it follows that $P_6(n)$ has at least one positive root. You can solve Equation $P_6(n) = 0$ for various values of Ta.

Ta	n
0	2.2214414690791653
10	2.2701220212994313
20	2.3152337874397433
30	2.357307022975578
40	2.3967590112653743
50	2.4339244154698263
60	2.4690760070425886
70	2.502439230663717
80	2.534202691665936
90	2.5645258696194655
100	2.59354489845482

Table 5.2: *Values of the critical wave number n for a range of values of Ta.*

Figure 5.6 shows an approximately linear relationship between the critical wave number n and the Taylor number Ta with the correlation coefficient ($r = 0.99677139$). Table (5.2) shows that the critical wave number n does not increase greatly as Ta goes from 0 to 100.

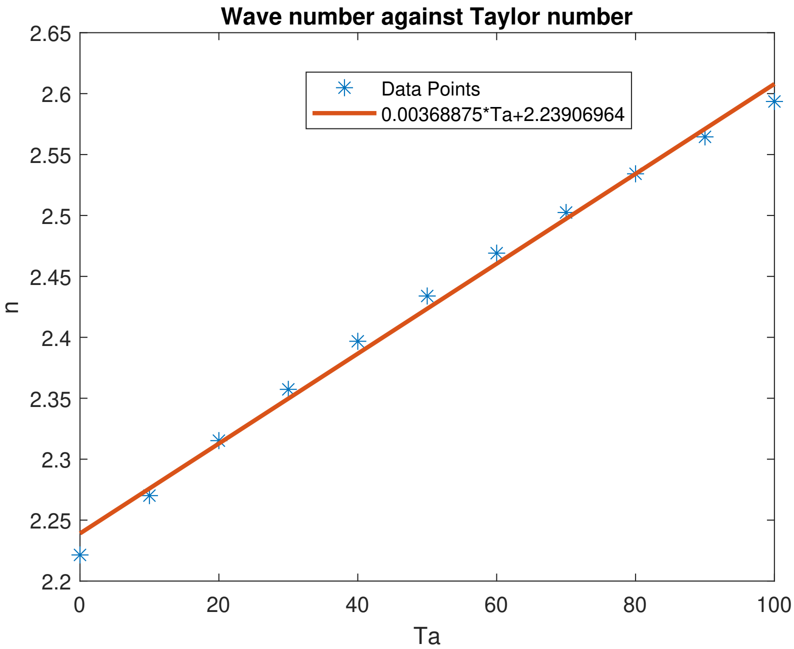

Figure 5.6: *The plot of $P_6(n)$ against n for a range of values on Ta. shows a linear relationship between the wavenumber n and the Taylor number Ta*

In Figure 5.7 we generate plots of R_T^{sc} against n for various combinations of Ta and Le. We maintain a constant value of $R_S = 100$ and assume no gravity modulation. The presence of gravity modulation impacts the stability of the process by delaying instability. Figure 5.7 reveals that gravity modulation influences the convection stability in the poles. Gravity modulation exhibits both stabilizing and destabilizing effects contingent on whether there is an increase or decrease in gravity. Furthermore, the Lewis number is insignificant in the presence of rotation. Lastly, the modulation amplitude seems to be stabilizing the system.

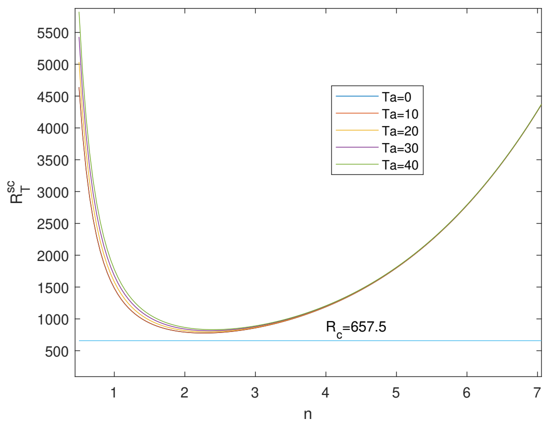

(a) Lewis number ($Le = 0.125$)

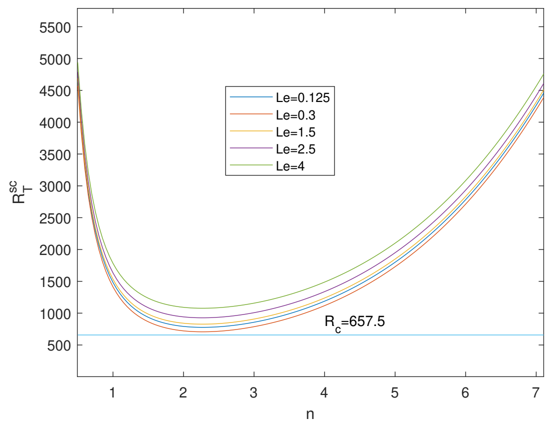

(b) $Ta = 30$

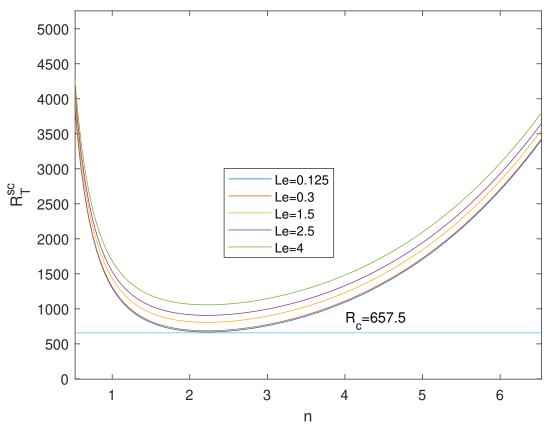

(c) No rotation

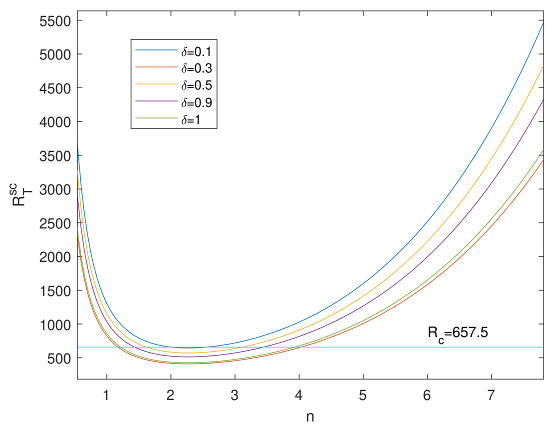

(d) At different values of δ.

Figure 5.7: *The Rayleigh number for stationary convection against the wave number (n) with and without rotation and different values of the Lewis number and the modulation amplitude.*

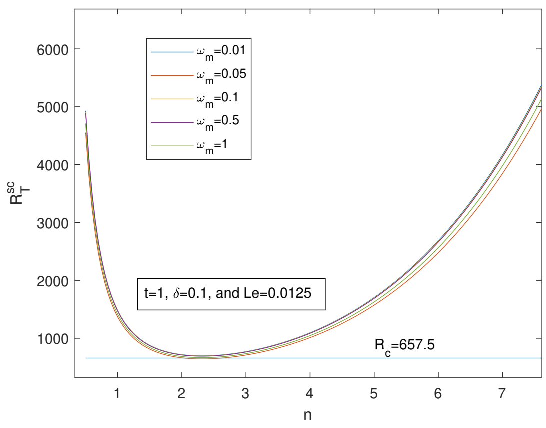

(a) $Ta = 30$

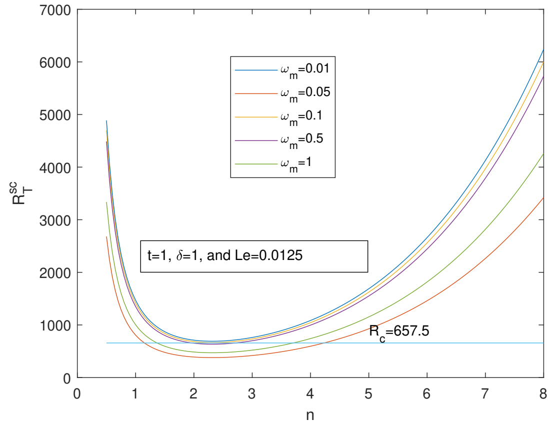

(b) $Ta = 30$

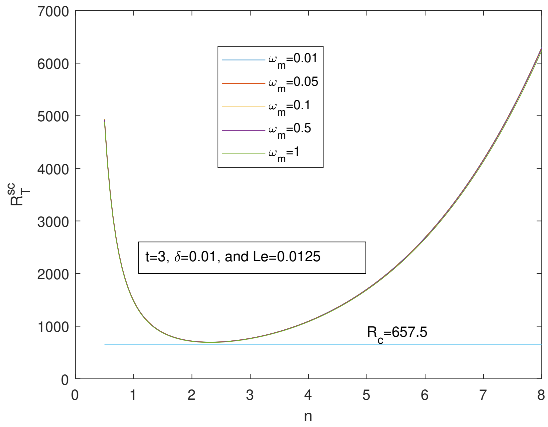

(c) $Ta = 30$

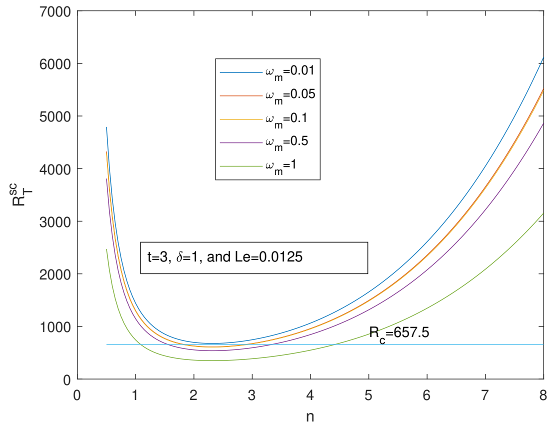

(d) $Ta = 30$

Figure 5.8: *The Rayleigh number for stationary convection plotted against the wave number (n) with gravity modulation and rotation using equation (5.18)*

Figure 5.8 indicates that gravity modulation through rotation significantly impacts stability, particularly for relatively high amplitudes of modulation. As such, it appears that the system tends to stabilize under conditions of elevated frequency. Conversely, negligible changes in stability are observed for minimal amplitudes of modulation. This underscores the critical role of gravity modulation in influencing system dynamics, particularly in contexts characterized by substantial amplitude variations.

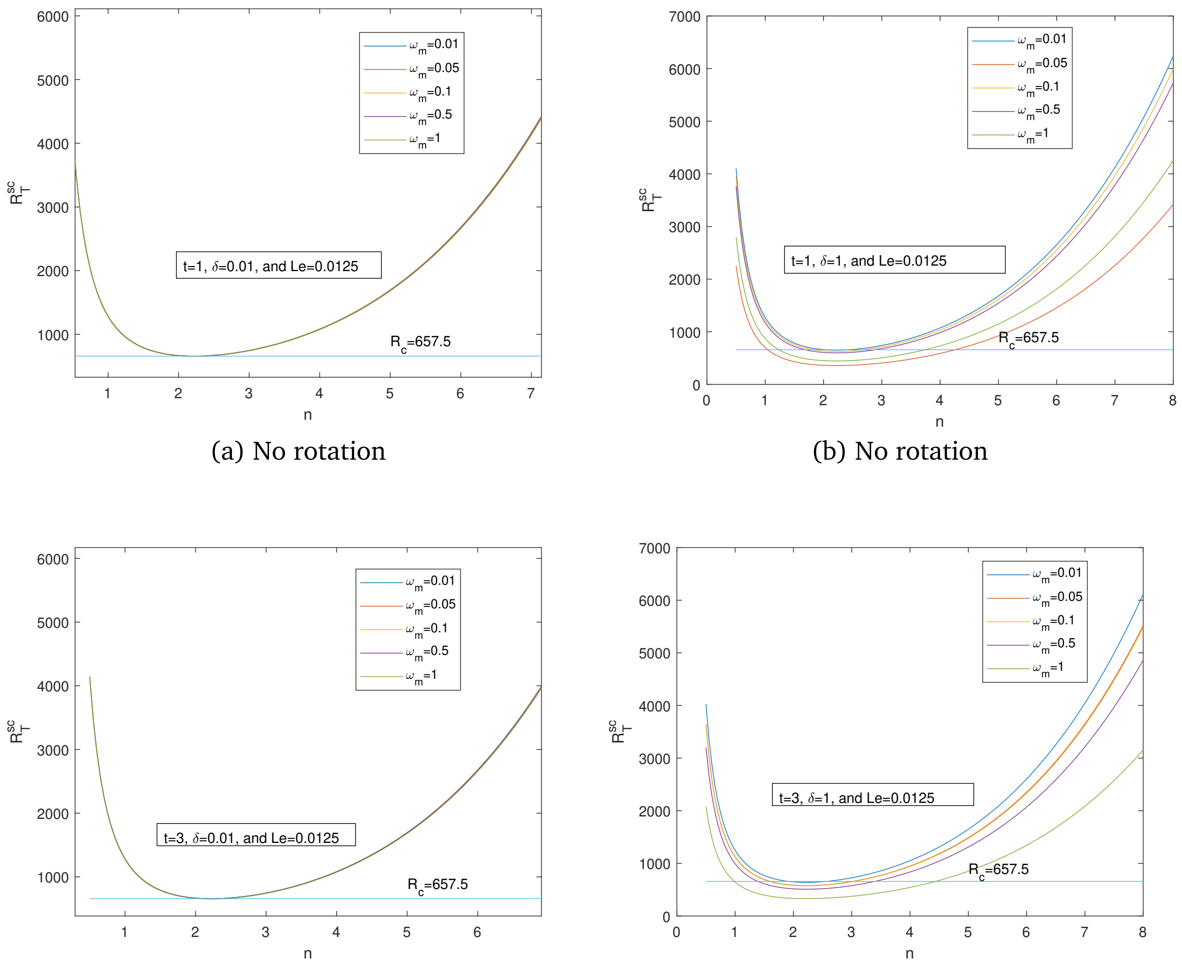

(a) No rotation

(b) No rotation

(c) No rotation

(d) No rotation

Figure 5.9: *The Rayleigh number against the wave number with gravity modulation and no rotation.*

In Figures 5.8 and 5.9 outcomes regarding the influence of modulation amplitude and frequency on convection in the absence of rotation mirror those observed in the rotating system. However, a notable distinction lies in the relatively high values of the Rayleigh number within the rotating system. This discrepancy highlights the significance of rotational effects on the convective dynamics, suggesting a significant interplay between modulation parameters and system behavior.

5.5 Summary

In this chapter, the focus was on stationary convection. In this type of stability analysis, we set the growth rate, σ, to zero in equation (4.101). We conducted stability analysis at both the poles and the equator. At the equator, the smaller the wave number (n), the higher the Rayleigh number, hence an unstable system. Additionally, there is no actual effect between rotation and gravity modulation. Also, minor changes in gravity modulation significantly affect the Rayleigh number. At the poles, we found that higher modulated amplitude causes the system to be unstable while higher modulated frequencies stabilize the system.

Chapter 6

Oscillatory convection

6.1 Introduction

Similar to the stability analysis conducted in Chapter 5 where we have considered stationary convection. Here we have assumed the growth rate to be non-zero. We now let $\sigma = \sigma_I$, where σ_I signifies the imaginary part of the growth. We again consider equation (4.101) for the Rayleigh number. We then substitute $\sigma = \sigma_I$ and compute R_{oc} with the critical Rayleigh number ($R_c = 27\pi^4/4$). We again conduct stability analysis at the poles and the equator. we will again vary the different parameters.

6.2 Analysis

Oscillatory motions occur when conditions such as salinity gradient, magnetic field, and rotation are present. Consider the mode,

$$\sigma_I = \lambda,$$

from equation (4.101) where λ is the oscillation frequency. We impose that $\lambda^2 > 0$ such that λ is real and we can obtain over stability. Substituting $\sigma = i\lambda$ into equation (4.101) yields two equations (real and imaginary). We need the equations to vanish separately. Thus, we can obtain solutions to the characteristic values of the oscillation frequency and the Rayleigh number. Therefore, equation (4.101) reduces to,

$$R_T^{Oc} = \frac{b_0 i\lambda + c_1}{n^2 g(t)} + \frac{b_1 i\lambda + c_2}{n^2 g(t) c_0} + \frac{b_3 i\lambda + c_3}{c_4}, \tag{6.1}$$

where,

$$\begin{array}{lll} m^2 = \pi^2 + n^2, & c_0 = m^4 + \lambda^2 Pr^{-2}, & c_1 = m^6 - \lambda^2 m^2 Pr^{-1}, \\ c_2 = \left(m^4 + \lambda^2 Pr^{-1}\right) Ta\Theta, & c_3 = \left(m^4 Le + \lambda^2 Le^2\right) R_S, & c_4 = m^4 + Le^2\lambda^2, \\ b_0 = m^4\left(1 + Pr^{-1}\right), & b_1 = Ta\Theta\left(m^2 - Pr^{-1}m^2\right), & b_3 = m^2\left(1 - Le\right) R_S Le. \end{array}$$

Equation (6.1) can further be reduced to,

$$R_T^{Oc} = \chi_r + i\lambda\chi_i, \tag{6.2}$$

where,

$$\chi_r = \frac{c_0c_1c_4 + c_2c_4 + c_0c_3n^2g(t)}{c_0c_4n^2g(t)},$$
$$\chi_i = \frac{c_0c_4b_0 + c_4b_1 + c_0b_3n^2g(t)}{c_0c_4n^2g(t)}.$$

We require R_T^{Oc} to be real [6] so that we interpret the results of the analysis in terms of real physical processes, like the onset of convection. Therefore, $\chi_i = 0$ in equation (6.2). That is,

$$\frac{c_0c_4b_0 + c_4b_1 + c_0b_3n^2g(t)}{c_0c_4n^2g(t)} = 0, \tag{6.3}$$

or simply

$$c_0c_4b_0 + c_4b_1 + c_0b_3n^2g(t) = 0. \tag{6.4}$$

Equation (6.4) can be written as a second-order polynomial in λ^2

$$(\lambda^2)^2 + B\lambda^2 + C = 0, \tag{6.5}$$

where

$$\begin{aligned} B = (\pi^2+n^2)&\left[(\pi^2+n^2)(Pr^2+Le^{-2})\right] \\ &+ (\pi^2+n^2)\left[Pr(Pr-1)Ta(k_y\cos^2\theta + (\pi^2+n^2)\pi^2\sin^2\theta)\right] \\ &+ (\pi^2+n^2)\left[n^2(1-Le)Le^{-1}\ R_S\ g_1(t)\right], \end{aligned} \tag{6.6}$$

and

$$\begin{aligned} C = (\pi^2+n^2)^3&\left[(\pi^2+n^2)Pr^2\ Le^{-2}\right] \\ &+ (\pi^2+n^2)^3\left[Pr\ Le^{-2}(Pr-1)Ta(k_y\cos^2\theta + \pi^2\sin^2\theta)\right] \\ &+ (\pi^2+n^2)^3\left[n^2Pr^2(1-Le)Le^{-1}\ R_Sg_1(t)\right]. \end{aligned} \tag{6.7}$$

λ^2 is the smallest positive root of dispersion. Thus,

$$R_T^{Oc} = \frac{c_0c_1c_4 + c_2c_4 + c_0c_3n^2g(t)}{c_0c_4n^2g(t)}. \tag{6.8}$$

6.3 Oscillatory convection at the equator

Consider the plot of the equation (6.8) against various parameters for different values of Ta. At the equator ($\theta = 0$), we have $\Theta = k_y$, thus, consequently leading to the following. We set $R_S = 100$, $Le = 20$, $Pr = 7$, $\Theta = k_y = 0.1$ and we set $\lambda = 0.1$ to obtain results for the analysis unless stated otherwise.

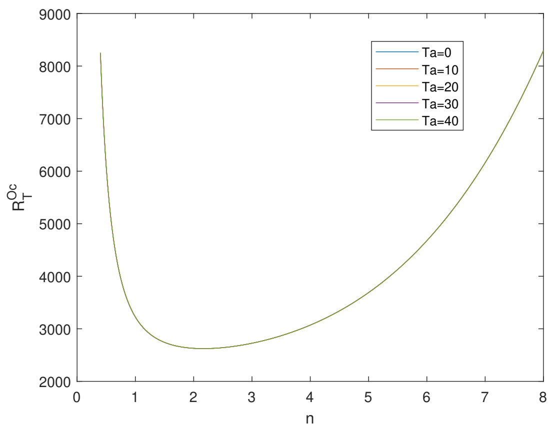

(a) No gravity modulation

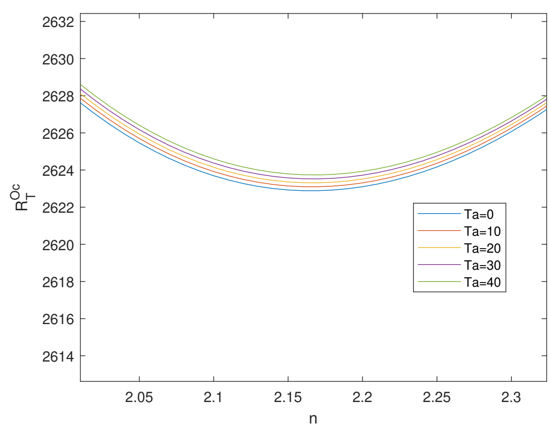

(b) No gravity modulation

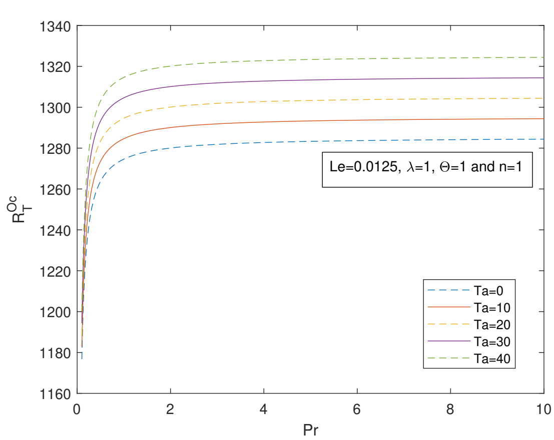

(c) No gravity modulation

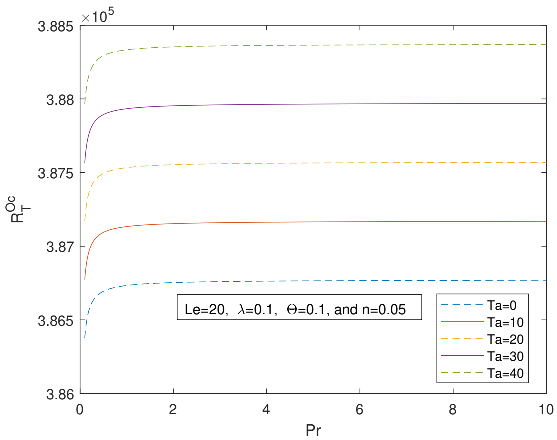

(d) No gravity modulation

Figure 6.1: *The Rayleigh number for oscillatory convection plotted against the wave number (n) and plotted against the Prandtl number (Pr).*

From Figure 6.1 above, it is apparent that in equatorial regions, the influence of the horizontal wave number in the y direction k_y significantly impacts stability, with rotation playing a minor role in these areas (Figures See 6.1 (c) and (d)). Furthermore, the importance of the diffusivity ratio Le between heat and salt to stability becomes evident as Pr varies. Higher values of Le lead to increased values of the Rayleigh number, and conversely, lower values of Le result in reduced instability.

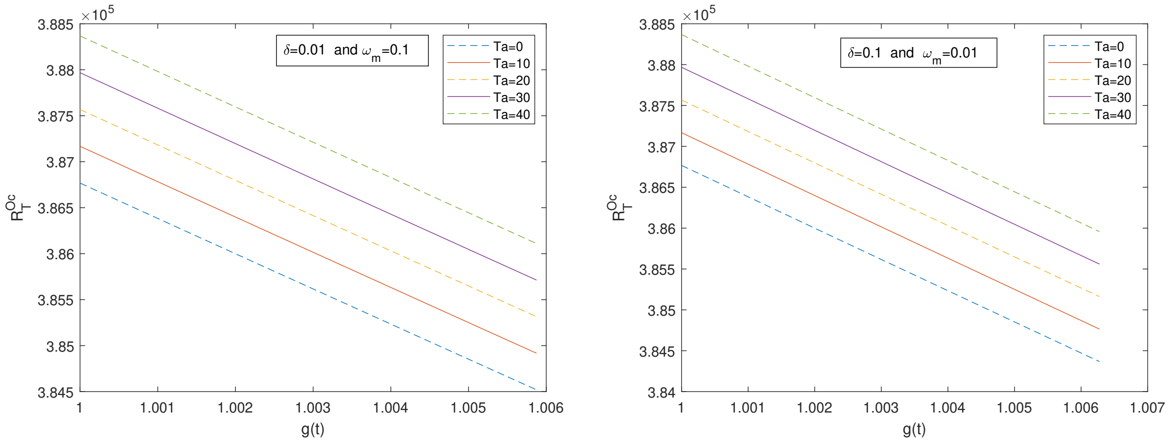

(a) $\delta = 0.01$ and $\omega_m = 0.1$ (b) $\delta = 0.1$ and $\omega_m = 0.01$

Figure 6.2: *The Rayleigh number for oscillatory convection plotted against gravity modulation at fixed amplitude and frequency values.*

From Figure 6.1 it is evident that in oscillatory convection, the modulation of gravity exhibits signs of both stabilizing and destabilizing effects. The system's stability depends on whether $g(t)$ exceeds or falls below one. This outcome suggests gravity modulation significantly influences the system's stability despite the relatively small variations.

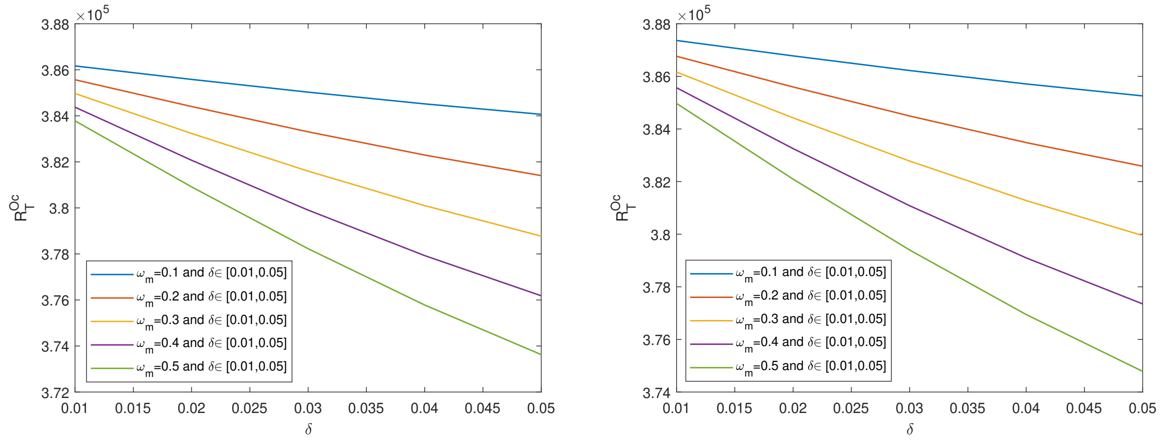

(a) No rotation (b) $Ta = 30$

Figure 6.3: *The Rayleigh number for oscillatory convection plotted against amplitude at fixed frequency values with and without rotation.*

From Figure 6.3 it is evident that in the presence of gravity modulation, varying the modulation amplitude (δ) at different modulation frequencies (ω_m) results in remarkably similar behaviors, in the presence of rotation and its absence. A similar result occurs when we vary ω_m for different values of δ (See Figure 6.4). It is crucial to highlight that the presence of gravity modulation yields relatively high values of the Rayleigh number, with further amplification when the system incorporates rotation.

This deduction leads us to infer that in equatorial regions, under the influence of both gravity modulation and rotation, the system exhibits a relatively heightened state of instability.

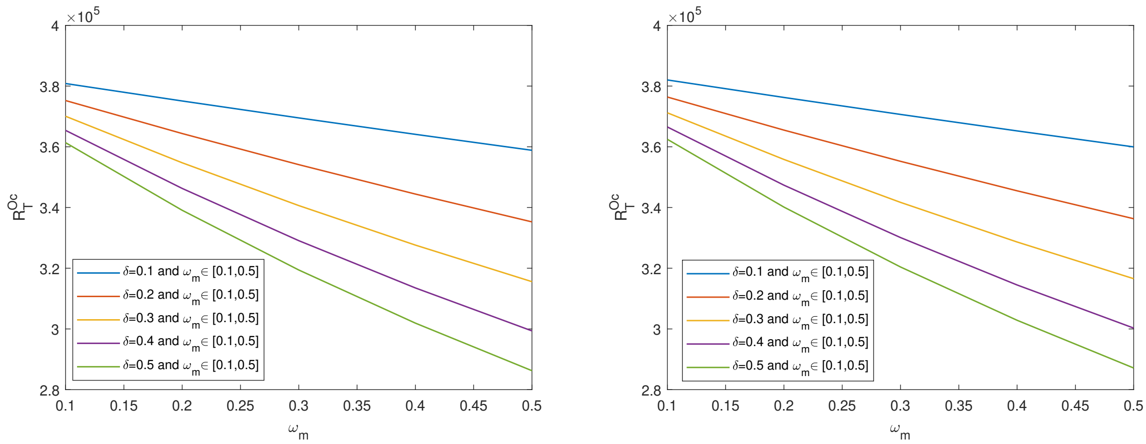

(a) No rotation (b) With rotation

Figure 6.4: *The Rayleigh number for oscillatory convection plotted against frequency at fixed amplitude values with and without rotation.*

6.4 Oscillatory convection at the poles

Let us consider the scenario where $\theta = \pi/2$ (at the poles). In this case, $\Theta = \pi^2$. We keep certain parameters constant while adjusting others to discern the relationships between them and their impact on convection. The results are outlined as follows:

From Figure 6.5, it becomes evident that rotation assumes a markedly more substantial role in convection, even without gravity modulation. Within these areas, convection processes exhibit a higher sensitivity to rotation compared to the **equatorial** regions. This observation may be linked to the poles serving as our planet's rotation axis. The simultaneous variation of both horizontal wave numbers could also contribute to this heightened sensitivity.

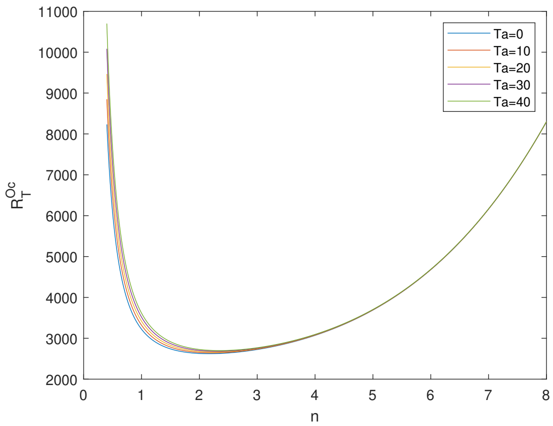

(a) No gravity modulation

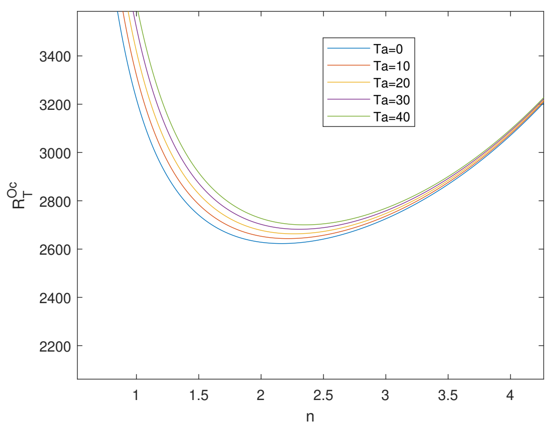

(b) No gravity modulation

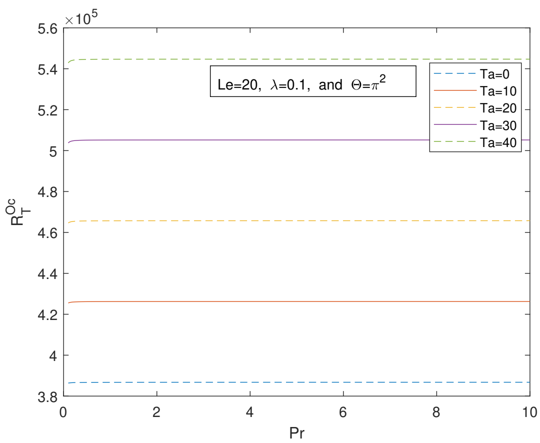

(c) No gravity modulation

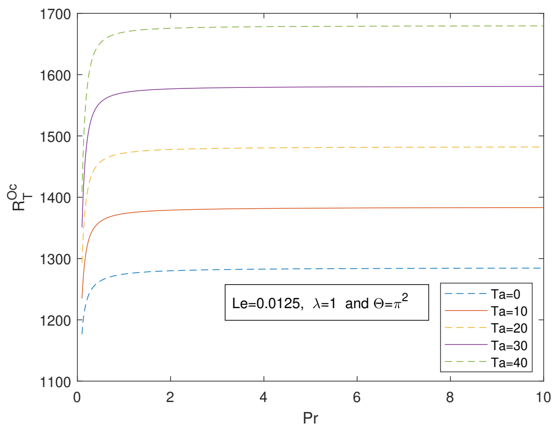

(d) No gravity modulation

Figure 6.5: *Rayleigh number for oscillatory convection plotted against wave-number, and Prandtl number without gravity modulation.*

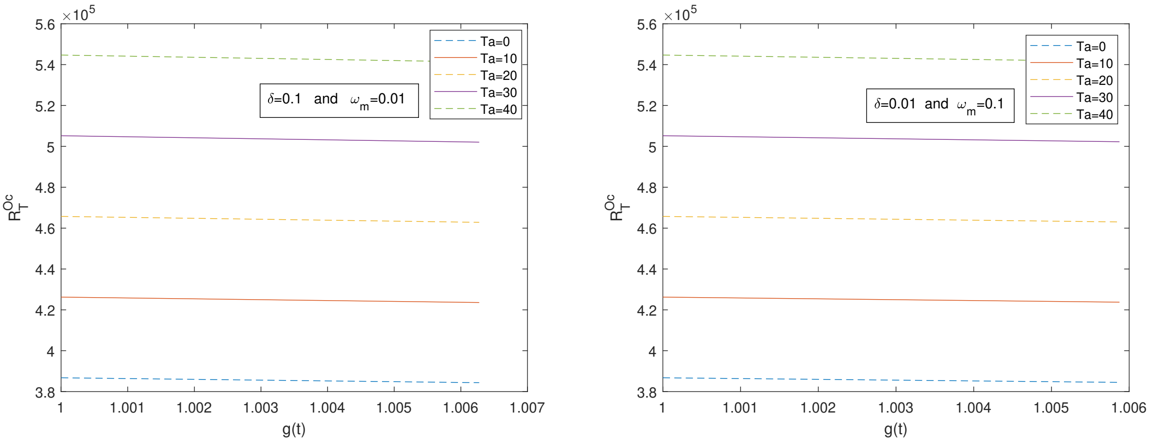

(a) $\delta = 0.1$ and $\omega_m = 0.01$

(b) $\delta = 0.01$ and $\omega_m = 0.1$

Figure 6.6: *The Rayleigh number for oscillatory convection against gravity modulation at fixed values of frequency and amplitude.*

From Figure 6.6 we can deduce that similar to the equatorial regions, the Lewis number (Le) is a significant factor influencing convection when investigating the relationship between the Prandtl number (Pr) and the Rayleigh number. Rotation continues to exert a pivotal influence in this context. The system exhibits indications of instability with an increase in the Taylor number (Ta). Additionally, akin to the equatorial regions, the presence of gravity modulation influences the convection process in the system. However, notable differences arise as gravity modulation in the polar regions generates higher Rayleigh numbers compared to the equatorial regions.

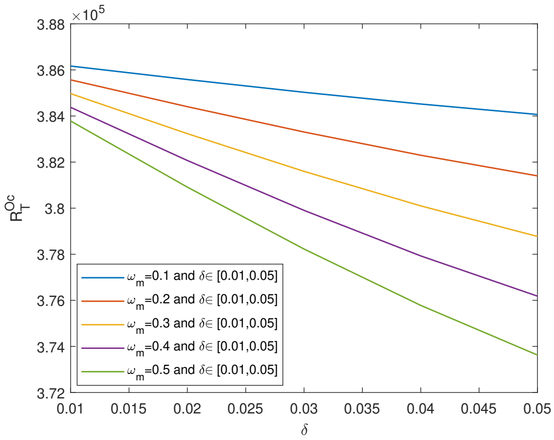

(a) No rotation

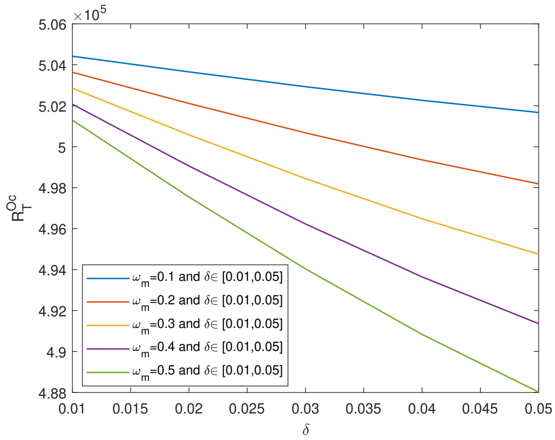

(b) Ta=20

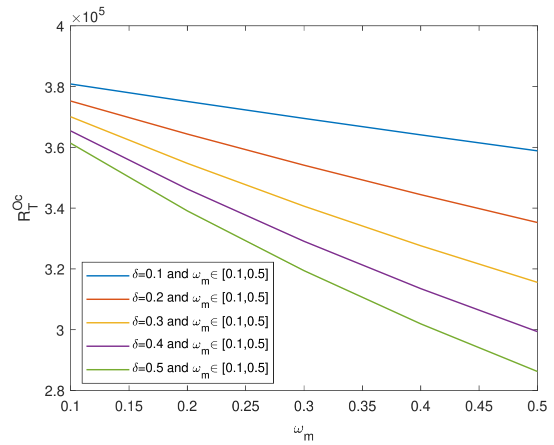

(c) No rotation

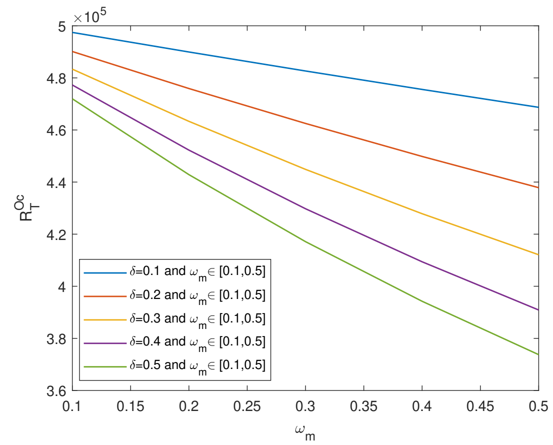

(d) Ta=20

Figure 6.7: *The Rayleigh number for oscillatory convection plotted against the modulation amplitude, and the Rayleigh number against the modulation frequency.*

Including rotation along with amplitude and frequency modulation results in higher Rayleigh numbers compared to the scenario without rotation (See Figure 6.7). This observation implies that the introduction of rotation introduces a new dynamic regarding system stability. The system appears to be unstable whenever rotation and gravity modulation coexist.

Parallel to the preceding analysis, the polar regions demonstrate relatively high Rayleigh numbers. This distinction becomes evident only when the system incorporates rotation. The sole contrast between the polar and equatorial regions lies in the value of Θ. This implies that for $k_y = \pi^2$ in the equatorial regions, a comparable behavior is anticipated to occur as observed in the polar regions.

6.5 Summary

The non-zero growth rare condition in this chapter led us to oscillatory convection and we conducted a stability analysis thereof. With a complex number growth rate ($\sigma = i\lambda$) we expect to observe some oscillations and hence we substituted this in equation (4.101). Similar to the previous chapter, our focus was on the poles and the equator. On the poles, Figure 6.5 suggests that rotation plays a very important role in stability analysis. Figure 6.6 shows that gravity modulation is directly proportional to the Rayleigh number. In the equator, Figure 6.1 demonstrates that gravity modulation affects the stability of the system.

Chapter 7

Summary and Conclusions

In summary, our investigation focused on the effects of gravity modulation on double-diffusive convection in rotating fluids such as the stratified ocean, which is heated from below. The method of normal modes has been used to study the linear problem and thereby conduct a linear stability analysis.

Due to the rotating nature of our problem, two very important concepts needed to be introduced. First is the rotating axis theorem to transition from the inertial frame to a rotating frame, and second is the no-traditional approximation of the Coriolis effect. By doing so, two fictitious forces were introduced into the momentum equation, the Coriolis force and the centrifugal force. The Coriolis force plays a very active role whereas the centrifugal force is absorbed into the pressure term and does not explicitly interact as much with the system. We conducted stability analysis for both stationary and oscillatory convection. The analysis was conducted in both polar regions and equatorial regions. Due to high temperatures, and glaciers melting, the ocean experiences mass re-distribution which creates gravity variations in the ocean.

For stationary convection, the following results were obtained.

- The smaller the wave number (n), the higher the Rayleigh number and consequently the unstable regime.
- Minor changes in gravity modulation have a significant effect on stability.

In the polar regions, the higher the amplitude of the modulation, the greater the Rayleigh number, whereas the frequency of modulation has stabilizing effects.

For oscillatory convection, the following results were obtained.

- At high latitudes, rotational effects are very significant. Furthermore, an increase in gravity modulation causes an increase in the Rayleigh number.
- In the equatorial regions, our results show that gravity modulation significantly affects the stability of ocean convection.

Distinct behaviors were evident between equatorial and polar regions, with polar regions typically exhibiting higher Rayleigh numbers, especially under rotational effects. This spatial variation underscores the importance of considering environmental conditions when analyzing convective processes. Moreover, our investigation emphasized the significance of wave direction, particularly near the equator, where the horizontal wave number in the $y-$ direction played a significant role. This aspect adds another layer of complexity to convective dynamics, influencing stability patterns in conjunction with other factors.

In conclusion, the study advances the understanding of convective stability by highlighting the interactions among the Rayleigh number, Lewis number, gravity modulation, rotation, Prandtl number, and wave directionality. By examining these factors, we enhance our ability to predict and interpret convective behaviors across diverse environmental conditions. The coexistence of rotation and gravity modulation suggests a higher likelihood of system instability. Amplitude and frequency modulations also play crucial roles in convection, particularly rotation. Rotation, in general, induces elevated values of the Rayleigh number, highlighting its substantial influence on the system.

Bibliography

[1] S. Chandrasekhar, “Thermal convection,” *Daedalus*, vol. 86, no. 4, pp. 323–339, 1957.

[2] R. M. Fand and K. K. Keswani, “Combined natural and forced convection heat transfer from horizontal cylinders to water,” *International Journal of Heat and Mass Transfer*, vol. 16, no. 6, pp. 1175–1191, 1973.

[3] P. G. Siddheshwar and S. Pranesh, “Effect of temperature/gravity modulation on the onset of magneto-convection in weak electrically conducting fluids with internal angular momentum,” *Journal of Magnetism and Magnetic Materials*, vol. 192, no. 1, pp. 159–176, 1999.

[4] C. A. Vreugdenhil and B. Gayen, “Ocean convection,” *Fluids*, vol. 6, no. 10, p. 360, 2021.

[5] D. Bouffard and A. Wüest, “Convection in lakes,” *Annual Review of Fluid Mechanics*, vol. 51, pp. 189–215, 2019.

[6] S. F. Chandrasekhar, “Hydrodynamic and hydromagnetic stability,” 1961.

[7] P. G. Drazin and W. H. Reid, *Hydrodynamic stability*. Cambridge University Press, 2004.

[8] L. Rayleigh, “LIX. on convection currents in a horizontal layer of fluid, when the higher temperature is on the underside,” *The London, Edinburgh, and Dublin Philosophical Magazine and Journal of Science*, vol. 32, no. 192, pp. 529–546, 1916.

[9] J. S. Turner and H. Stommel, “A new case of convection in the presence of combined vertical salinity and temperature gradients,” *Proceedings of the national academy of sciences*, vol. 52, no. 1, pp. 49–53, 1964.

[10] M. E. Stern, “The ‘salt-fountain’ and thermohaline convection,” *Tellus*, vol. 12, no. 2, pp. 172–175, 1960.

[11] C. Eckart, *Hydrodynamics of oceans and atmospheres*. Elsevier, 2013.

[12] G. Walin, “Note on the stability of water stratified by both salt and heat,” *Tellus*, vol. 16, no. 3, pp. 389–393, 1964.

[13] G. Veronis, “Penetrative convection.” *The Astrophysical Journal*, vol. 137, pp. 641–645, 1963.

[14] G. Veronis and G. Veronis, "On finite amplitude instability in thermohaline convection," *Journal of Marine Research*, vol. 23, no. 1, pp. 1–17, 1965.

[15] D. A. Nield, "The thermohaline Rayleigh-Jeffreys problem," *Journal of Fluid Mechanics*, vol. 29, no. 3, pp. 545–558, 1967.

[16] P. G. Baines and A. E. Gill, "On thermohaline convection with linear gradients," *Journal of Fluid Mechanics*, vol. 37, no. 2, pp. 289–306, 1969.

[17] A. L. Gordon, "South Atlantic thermocline ventilation," *Deep Sea Research Part A. Oceanographic Research Papers*, vol. 28, no. 11, pp. 1239–1264, 1981.

[18] J. Marshall and R. A. Plumb, *Atmosphere, ocean and climate dynamics: An introductory text*. Academic Press, 1989.

[19] P. F. Linden and T. G. L. Shirtcliffe, "The diffusive interface in double-diffusive convection," *Journal of Fluid Mechanics*, vol. 87, no. 3, pp. 417–432, 1978.

[20] E. Hage and A. Tilgner, "High Rayleigh number convection with double diffusive fingers," *Physics of Fluids*, vol. 22, no. 7, pp. 076 603–076 612, 2010.

[21] T. J. McDougall, "Double-diffusive convection caused by coupled molecular diffusion," *Journal of Fluid Mechanics*, vol. 126, pp. 379–397, 1983.

[22] M. Yoshida and A. Kageyama, "Application of the Yin-Yang grid to a thermal convection of a Boussinesq fluid with infinite Prandtl number in a three-dimensional spherical shell," *Geophysical Research Letters*, vol. 31, no. 12–28, 2004.

[23] E. A. Spiegel and G. Veronis, "On the Boussinesq approximation for a compressible fluid." *The Astrophysical Journal*, vol. 131, pp. 442–448, 1960.

[24] B. Gayen and R. W. Griffiths, "Rotating horizontal convection," *Annual Review of Fluid Mechanics*, vol. 54, pp. 105–132, 2022.

[25] A. J. Barker, A. M. Dempsey, and Y. Lithwick, "Theory and simulations of rotating convection," *The Astrophysical Journal*, vol. 791, no. 1, pp. 13–22, 2014.

[26] P. Billant, "Is the Taylor-Proudman theorem exact in unbounded domains? Case study of the three-dimensional stability of a vortex pair in a rapidly rotating fluid," *Journal of Fluid Mechanics*, vol. 920, p. R1, 2021.

[27] K. Julien, S. Legg, J. McWilliams, and J. Werne, "Rapidly rotating turbulent Rayleigh-Bénard convection," *Journal of Fluid Mechanics*, vol. 322, pp. 243–273, 1996.

[28] S. M. Cox and P. C. Matthews, "Instability of rotating convection," *Journal of Fluid Mechanics*, vol. 403, pp. 153–172, 2000.

[29] E. M. King, S. Stellmach, and J. M. Aurnou, "Heat transfer by rapidly rotating Rayleigh-Bénard convection," *Journal of Fluid Mechanics*, vol. 691, pp. 568–582, 2012.

[30] P. Vorobieff and R. E. Ecke, "Turbulent rotating convection: An experimental study," *Journal of Fluid Mechanics*, vol. 458, pp. 191–218, 2002.

[31] T. Gerkema, J. Zimmerman, L. Maas, and H. Van Haren, "Geophysical and astrophysical fluid dynamics beyond the traditional approximation," *Reviews of Geophysics*, vol. 46, no. 2, 2008.

[32] C. T. Duba, M. Shekar, M. Narayana, and P. Sibanda, "Soret and Dufour effects on thermohaline convection in rotating fluids," *Geophysical & Astrophysical Fluid Dynamics*, vol. 110, no. 4, pp. 317–347, 2016.

[33] G. Venezian, "Effect of modulation on the onset of thermal convection," *Journal of Fluid Mechanics*, vol. 35, no. 2, pp. 243–254, 1969.

[34] T. Radko, *Double-diffusive convection*. Cambridge University Press, 2013.

[35] P. Garaud, "Double-diffusive convection at low Prandtl number," *Annual Review of Fluid Mechanics*, vol. 50, pp. 275–298, 2018.

[36] T. M. Johnston, D. L, and E. Pallàs-Sanz, "Elevated mixing at a front," *Journal of Geophysical Research: Oceans*, vol. 116, no. C11, 2011.

[37] P. G. Siddheshwar, B. S. Bhadauria, and A. Srivastava, "An analytical study of nonlinear double-diffusive convection in a porous medium under temperature/gravity modulation," *Transport in Porous Media*, vol. 91, no. 2, pp. 585–604, 2012.

[38] P. Vadasz, "Coriolis effect on gravity-driven convection in a rotating porous layer heated from below," *Journal of Fluid Mechanics*, vol. 376, pp. 351–375, 1998.

[39] M. S. Malashetty and V. Padmavathi, "Effect of gravity modulation on the onset of convection in a fluid and porous layer," *International Journal of Engineering Science*, vol. 35, no. 9, pp. 829–840, 1997.

[40] B. S. Bhadauria and P. Kiran, "Weak nonlinear double diffusive magneto-convection in a Newtonian liquid under gravity modulation," *Journal of Applied Fluid Mechanics*, vol. 8, no. 4, pp. 735–746, 2015.

[41] P. Kiran, S. H. Manjula, and R. Roslan, "The effect of gravity modulation on double diffusive convection in the presence of applied magnetic field and internal heat source," *Advanced Science, Engineering and Medicine*, vol. 12, no. 6, pp. 792–805, 2020.

[42] P. Kiran, "G-jitter effects on chaotic convection in a rotating fluid layer," *Advances in Condensed-Matter and Materials Physics-Rudimentary Research to Topical Technology*, 2020.

[43] P. Kiran and P. Kiran, "Gravity modulation effect on weakly nonlinear thermal convection in a fluid layer bounded by rigid boundaries," *International Journal of Nonlinear Sciences and Numerical Simulation*, vol. 24, no. 3, pp. 867–881, 2023.

[44] B. S. Bhadauria and K. Palle, "Weak nonlinear oscillatory convection in a viscoelastic fluid-saturated porous medium under gravity modulation," *Transport in Porous Media*, vol. 104, no. 3, pp. 451–467, 2014.

[45] R. A. Rohde and Z. Hausfather, "The Berkeley Earth land/ocean temperature record," *Earth System Science Data*, vol. 12, no. 4, pp. 3469–3479, 2020.

[46] B. D. Tapley, F. Flechtner, S. V. Bettadpur, and M. M. Watkins, "The status and future prospect for GRACE after the first decade," in *AGU Fall Meeting Abstracts*, vol. 2013, 2013, pp. G32A–01.

[47] G. W. Platzman, "The spectral dynamics of laminar convection," *Journal of Fluid Mechanics*, vol. 23, no. 3, pp. 481–510, 1965.

[48] A. F. Vakakis, "Analysis and identification of linear and nonlinear normal modes in vibrating systems," Ph.D. dissertation, California Institute of Technology, 1991.

[49] L. Manevich and I. V. Mikhlin, "On periodic solutions close to rectilinear normal vibration modes," *Journal of Applied Mathematics and Mechanics*, vol. 36, no. 6, pp. 988–994, 1972.

[50] J. C. Slater, "A numerical method for determining nonlinear normal modes," *Nonlinear Dynamics*, vol. 10, no. 1, pp. 19–30, 1996.

[51] G. M. Mirouh, P. Garaud, S. Stellmach, A. L. Traxler, and T. S. Wood, "A new model for mixing by double-diffusive convection (semi-convection). The conditions for layer formation," *The Astrophysical Journal*, vol. 750, no. 1, p. 61, 2012.

[52] B. M. Shankar, J. Kumar, and I. S. Shivakumara, "Stability of double-diffusive natural convection in a vertical fluid layer," *Physics of Fluids*, vol. 33, no. 9, 2021.

[53] G. K. Vallis, *Atmospheric and oceanic fluid dynamics*. Cambridge University Press, 2017.

[54] W. Chen and C. F. Chen, "Effect of gravity modulation on the stability of convection in a vertical slot," *Journal of Fluid Mechanics*, vol. 395, pp. 327–344, 1999.